HE4 in PR patients was significantly lower than that in PD patients ($p<0.001$) (Fig. 4a). Overall median survival after treatment was 9.6 months. Post-treatment HE4 levels were above the cutoff limit (15 ng/ml) in one of eight for PR and in four of five for PD patients. We divided patients into high (>15 ng/ml) and low (<15 ng/ml) HE4 groups post-treatment. We set the cutoff point at 15 ng/ml based on the median value of HE4 levels. Median overall survival of low HE4 group was significantly longer than that of high HE4 group (17.3 vs. 7.7 months; $p<0.05$) (Fig. 4b). Median progression-free survival after chemotherapy for low HE4 group was 2.4 months, compared with 1.4 months for high HE4 group ($p=0.083$) (Fig. 4b).

Discussion

In our study, we developed a novel ELISA system to detect serum HE4, and by using this system, we show that HE4 has potential as a diagnostic marker of lung cancer. Specifically, we found that serum HE4 levels in lung cancer patients after chemotherapy is strongly correlated with survival after the treatment.

Our HE4 ELISA shows better sensitivity for diagnosis of ovarian cancer than the existing HE4 ELISA kit. Furthermore, there are two advantages to our HE4 ELISA over the existing HE4 ELISA kit. First, while the existing ELISA kit is designed to use undiluted serum as the test sample, using our system, a small sample volume can be applied to our ELISA to detect HE4 in human serum. A diluted sample, maximally five times dilution, can be used in our assay system. This is of practical importance when simultaneous measures of other biomarkers are required from one serum sample. Second, a simpler and more rapid test is achieved using our HE4 ELISA. Test duration for our HE4 ELISA is approximately half of the time required by the existing HE4 ELISA kit. The existing HE4 ELISA kit requires a shaking procedure during reaction of antibody to the sample, while our new ELISA incubates the sample with antibody in a stationary condition. Thus, our HE4 ELISA does not require the purchase of specialized equipment for shaking incubation.

We evaluated the diagnostic efficacy of HE4 in lung, ovarian, gastric and colorectal cancer patients and found that HE4 indicated high sensitivity in lung cancer patients. Tissue expression of HE4 has been reported to be increased in pulmonary, ovarian and gastrointestinal carcinomas [15–18, 20, 21]. HE4 as a serum marker was mainly investigated in ovarian cancer patients and was shown to be a promising diagnostic marker [22]. We show that serum HE4 levels were significantly higher for not only ovarian cancer but also lung cancer patients than for healthy controls. Escudero et al. previously measured HE4 concentrations in patients with various types of malignant diseases and found that HE4 concentrations were abnormal primarily in gynecologic cancer and lung cancer [23]. Taken together, these data HE4 may be considered to be a potential diagnostic marker of lung cancer.

In this study, we found that post-treatment HE4 level is correlated with survival after chemotherapy. It was reported that high levels of serum HE4 is significantly correlated with worse prognosis in epithelial ovarian cancer patients [24]. Yamashita et al. reported that HE4 expression by immunohistochemistry staining is significantly correlated with prognosis in lung adenocarcinoma patients [25]. There is a growing need for diagnostic tools to estimate the prognosis of the patient, to monitor the treatment course and to early detect the response to therapy, which would help to optimize disease management on an individual basis. Our results suggest that serum HE4 is a promising prognostic marker. To our knowledge, this is the first time that the potential prognostic impact of serum HE4 in lung cancer patients has been investigated. We are aware of the small cohort of patients in this study, and thus, further study by larger scale prospective trials will be needed.

In conclusion, we used ELISA systems developed by us to detect significant differences in the levels of serum HE4 between lung cancer patients and normal controls. In addition, it is suggested that HE4 is correlated with prognosis after chemotherapy. We are planning a further study to evaluate serum HE4 for a diagnostic and prognostic marker by larger scale of patients.

Acknowledgments We appreciate Shintaro Nomura (Nagahama Institute of Bio-Science and Technology, Shiga, Japan) for providing helpful comments on immunohistochemical analysis, Barry Ripley for outstanding editing of the manuscript and Masako Ikeda for their technical assistance. We wish to thank Y. Ito, N. Kawakami and Y. Kanazawa for their secretarial assistance. This work was supported by a grant-in-aid from the Ministry of Health, Labour and Welfare, Japan.

Conflict of interest None.

References

1. Jemal A, Siegel R, Xu J, Ward E. Cancer statistics, 2010. CA Cancer J Clin. 2010;60:277–300.
2. Fruh M. The search for improved systemic therapy of non-small cell lung cancer—what are today's options? Lung Cancer. 2011;72:265–70.
3. Martini N, Kris MG, Gralla RJ, Bains MS, McCormack PM, Kaiser LR, Burt ME, Zaman MB. The effects of preoperative chemotherapy on the resectability of non-small cell lung carcinoma with mediastinal lymph node metastases (n2 m0). Ann Thorac Surg. 1988;45:370–9.
4. Shinkai T, Saijo N, Tominaga K, Eguchi K, Shimizu E, Sasaki Y, Fujita J, Futami H, Ohkura H, Suemasu K. Serial plasma carcinoembryonic antigen measurement for monitoring patients with advanced lung cancer during chemotherapy. Cancer. 1986;57:1318–23.

5. Pujol JL, Grenier J, Daures JP, Daver A, Pujol H, Michel FB. Serum fragment of cytokeratin subunit 19 measured by cyfra 21-1 immunoradiometric assay as a marker of lung cancer. Cancer Res. 1993;53:61–6.
6. Miyake Y, Kodama T, Yamaguchi K. Pro-gastrin-releasing peptide (31-98) is a specific tumor marker in patients with small cell lung carcinoma. Cancer Res. 1994;54:2136–40.
7. Kirchhoff C, Habben I, Ivell R, Krull N. A major human epididymis-specific cDNA encodes a protein with sequence homology to extracellular proteinase inhibitors. Biol Reprod. 1991;45:350–7.
8. Kirchhoff C. Molecular characterization of epididymal proteins. Rev Reprod. 1998;3:86–95.
9. Wang K, Gan L, Jeffery E, Gayle M, Gown AM, Skelly M, Nelson PS, Ng WV, Schummer M, Hood L, Mulligan J. Monitoring gene expression profile changes in ovarian carcinomas using cDNA microarray. Gene. 1999;229:101–8.
10. Schummer M, Ng WV, Bumgarner RE, Nelson PS, Schummer B, Bednarski DW, Hassell L, Baldwin RL, Karlan BY, Hood L. Comparative hybridization of an array of 21,500 ovarian cDNAs for the discovery of genes overexpressed in ovarian carcinomas. Gene. 1999;238:375–85.
11. Hough CD, Sherman-Baust CA, Pizer ES, Montz FJ, Im DD, Rosenshein NB, Cho KR, Riggins GJ, Morin PJ. Large-scale serial analysis of gene expression reveals genes differentially expressed in ovarian cancer. Cancer Res. 2000;60:6281–7.
12. Ono K, Tanaka T, Tsunoda T, Kitahara O, Kihara C, Okamoto A, Ochiai K, Takagi T, Nakamura Y. Identification by cDNA microarray of genes involved in ovarian carcinogenesis. Cancer Res. 2000;60:5007–11.
13. Welsh JB, Zarrinkar PP, Sapinoso LM, Kern SG, Behling CA, Monk BJ, Lockhart DJ, Burger RA, Hampton GM. Analysis of gene expression profiles in normal and neoplastic ovarian tissue samples identifies candidate molecular markers of epithelial ovarian cancer. Proc Natl Acad Sci U S A. 2001;98:1176–81.
14. Shridhar V, Lee J, Pandita A, Iturria S, Avula R, Staub J, Morrissey M, Calhoun E, Sen A, Kalli K, Keeney G, Roche P, Cliby W, Lu K, Schmandt R, Mills GB, Bast Jr RC, James CD, Couch FJ, Hartmann LC, Lillie J, Smith DI. Genetic analysis of early- versus late-stage ovarian tumors. Cancer Res. 2001;61:5895–904.
15. Schaner ME, Ross DT, Ciaravino G, Sorlie T, Troyanskaya O, Diehn M, Wang YC, Duran GE, Sikic TL, Caldeira S, Skomedal H, Tu IP, Hernandez-Boussard T, Johnson SW, O'Dwyer PJ, Fero MJ, Kristensen GB, Borresen-Dale AL, Hastie T, Tibshirani R, van de Rijn M, Teng NN, Longacre TA, Botstein D, Brown PO, Sikic BI. Gene expression patterns in ovarian carcinomas. Mol Biol Cell. 2003;14:4376–86.
16. Lu KH, Patterson AP, Wang L, Marquez RT, Atkinson EN, Baggerly KA, Ramoth LR, Rosen DG, Liu J, Hellstrom I, Smith D, Hartmann L, Fishman D, Berchuck A, Schmandt R, Whitaker R, Gershenson DM, Mills GB, Bast Jr RC. Selection of potential markers for epithelial ovarian cancer with gene expression arrays and recursive descent partition analysis. Clin Cancer Res. 2004;10:3291–300.
17. Drapkin R, von Horsten HH, Lin Y, Mok SC, Crum CP, Welch WR, Hecht JL. Human epididymis protein 4 (he4) is a secreted glycoprotein that is overexpressed by serous and endometrioid ovarian carcinomas. Cancer Res. 2005;65:2162–9.
18. Rosen DG, Wang L, Atkinson JN, Yu Y, Lu KH, Diamandis EP, Hellstrom I, Mok SC, Liu J, Bast Jr RC. Potential markers that complement expression of ca125 in epithelial ovarian cancer. Gynecol Oncol. 2005;99:267–77.
19. Hellstrom I, Raycraft J, Hayden-Ledbetter M, Ledbetter JA, Schummer M, McIntosh M, Drescher C, Urban N, Hellstrom KE. The he4 (wfdc2) protein is a biomarker for ovarian carcinoma. Cancer Res. 2003;63:3695–700.
20. Bingle L, Cross SS, High AS, Wallace WA, Rassl D, Yuan G, Hellstrom I, Campos MA, Bingle CD. Wfdc2 (he4): a potential role in the innate immunity of the oral cavity and respiratory tract and the development of adenocarcinomas of the lung. Respir Res. 2006;7:61.
21. Galgano MT, Hampton GM, Frierson Jr HF. Comprehensive analysis of he4 expression in normal and malignant human tissues. Mod Pathol. 2006;19:847–53.
22. Li J, Dowdy S, Tipton T, Podratz K, Lu WG, Xie X, Jiang SW. He4 as a biomarker for ovarian and endometrial cancer management. Expert Rev Mol Diagn. 2009;9:555–66.
23. Escudero JM, Auge JM, Filella X, Torne A, Pahisa J, Molina R. Comparison of serum human epididymis protein 4 with cancer antigen 125 as a tumor marker in patients with malignant and nonmalignant diseases. Clin Chem. 2011;57:1534–44.
24. Steffensen KD, Waldstrom M, Brandslund I, Jakobsen A. Prognostic impact of prechemotherapy serum levels of her2, ca125, and he4 in ovarian cancer patients. Int J Gynecol Canc. 2011;21:1040–7.
25. Yamashita S, Tokuishi K, Hashimoto T, Moroga T, Kamei M, Ono K, Miyawaki M, Takeno S, Chujo M, Yamamoto S, Kawahara K. Prognostic significance of he4 expression in pulmonary adenocarcinoma. Tumour Biol. 2011;32:265–71.

The American Journal of Pathology, Vol. 180, No. 1, January 2012

DOI: 10.1016/j.ajpath.2011.09.013

Growth Factors, Cytokines, and Cell Cycle Molecules

Blockade of Interleukin-6 Receptor Alleviates Disease in Mouse Model of Scleroderma

Shun Kitaba,* Hiroyuki Murota,* Mika Terao,* Hiroaki Azukizawa,* Fumitaka Terabe,† Yoshihito Shima,‡ Minoru Fujimoto,† Toshio Tanaka,‡ Tetsuji Naka,† Tadamitsu Kishimoto,§ and Ichiro Katayama*

From the Department of Dermatology, Course of Integrated Medicine and the Department of Respiratory Medicine, Allergy and Rheumatic Diseases,‡ Graduate School of Medicine, Osaka University, Osaka; the Laboratory for Immune Signal,† National Institute of Biomedical Innovation, Osaka; and the Laboratory of Immune Regulation,§ Osaka University Graduate School of Frontier Biosciences, Osaka, Japan*

Activation of fibroblasts by interleukin-6 (IL-6) is implicated in the pathogenesis of scleroderma, suggesting that the inhibition of fibroblast activation may be a promising scleroderma treatment. In this study, we used an IL-6 blocking antibody (Ab) and *Il-6* knockout (Il-6KO) mice to examine the role of IL-6 in the bleomycin (BLM)-induced mouse model of scleroderma. BLM was administered to C57BL/6 and *Il-6*KO mice to induce dermal sclerosis. BLM-treated and control phosphate-buffered saline-treated mice were treated with anti-mouse IL-6 receptor monoclonal Ab (MR16-1). Disease severity was evaluated by measuring dermal thickness and skin hardness, by counting the numbers of α-smooth muscle actin-positive cells and mast cells, and by examining the cutaneous draining lymph nodes. C57BL/6 mice with BLM induced scleroderma had elevated serum IL-6 levels and more severe dermal sclerosis than *Il-6*KO mice. Weekly administration of MR16-1, but not control Ab, prevented and improved dermal sclerosis, and also attenuated swelling of the draining lymph nodes. MR16-1 suppressed α-smooth muscle actin induction in IL-6–stimulated *Il-6*KO fibroblasts. Our results indicate that IL-6 contributes to BLM induced dermal sclerosis and that IL-6 receptor–specific monoclonal Ab may improve the symptoms of scleroderma by suppressing fibroblast activation. *(Am J Pathol 2012, 180:165–176; DOI: 10.1016/j.ajpath.2011.09.013)*

Patients with scleroderma frequently experience broad area skin sclerosis and internal organ involvement including pulmonary fibrosis, esophageal dysfunction, pulmonary arterial hypertension, renal crisis, and heart failure.[1] These symptoms dramatically affect the prognosis for scleroderma patients. Autoaggressive immunological activation and continuous activation of fibroblasts are the key components of scleroderma, yet the mechanisms underlying these are incompletely understood.

Several lines of evidence indicate that interleukin (IL)-6 contributes to the disease process in scleroderma. Serum IL-2, IL-4, IL-6, and tumor necrosis factor α levels are elevated in scleroderma.[2–6] Increased serum IL-6 levels are also observed in both scleroderma mouse models: the bleomycin (BLM)-induced scleroderma mouse and the type 1 tight-skin mouse (*Tsk1/+*).[7,8] At the cellular level, IL-6–producing T helper type 2 clones contribute to anti-DNA topoisomerase I autoantibody, a key autoantibody in scleroderma.[9] The point of action of IL-6 in scleroderma remains controversial, with some evidence suggesting the final maturation step of B cells[10] and/or activation of fibroblasts.[11–13] Thus, although the specific function of IL-6 in the pathogenesis of scleroderma remains unclear, there is ample evidence that inhibition of IL-6–mediated signaling might be a route to better treatment for scleroderma.

In this study, we used the BLM-induced scleroderma mouse model to demonstrate the importance of IL-6 in pathogenesis of scleroderma and to evaluate the effect of anti-mouse IL-6 receptor monoclonal antibody. We have examined whether MR16-1 acts directly on dermal fibroblasts by investigating the induction of myofibroblasts *in vitro*. We also examined the tissue of scleroderma patients treated with tocilizumab, a humanized monoclonal antibody (Ab) against the IL-6 receptor used to treat rheumatoid arthritis or Castleman's disease.[14] Patients

Supported by the Program for Promotion of Fundamental Studies in Health Sciences of the National Institute of Biomedical Innovation.

Accepted for publication September 21, 2011.

Disclosure: T.K. holds a patent for tocilizumab. All other authors have no conflicts of interest to declare.

Address for reprint requests: Hiroyuki Murota, M.D., Ph.D., 2-2, Yamadaoka, Suita-Shi, Osaka, Japan 565-0871. E-mail: h-murota@derma.med.osaka-u.ac.jp.

with intractable scleroderma treated with tocilizumab were previously reported to show marked amelioration of dermal sclerosis.[15] Our results indicate that IL-6 induces dermal sclerosis via direct activation of dermal fibroblasts and that biomolecular targeting to suppress IL-6 might be a promising therapeutic approach for scleroderma.

Materials and Methods

Dermal Fibroblast Isolation and Culture

The dermis was collected and separated from the epidermis as described previously.[4,16] Briefly, newborn wild-type and *Il-6* knockout (KO) mouse pups (age 2 to 4 days) were sacrificed and rinsed in 70% ethanol. The skin was excised and treated with 4 mg/mL of dispase (Gibco, Invitrogen, Paisley, UK) for 1 hour at 37°C. The dermis was then separated from the epidermis, placed in phosphate-buffered saline (PBS) + 0.05% type-1 collagenase (Sigma-Aldrich, St. Louis, MO), and incubated at 37°C for 30 minutes with vigorous agitation to prepare single cells. After filtration, cells were resuspended in Dulbecco's modified Eagle's medium + 10% fetal bovine serum and incubated at 37°C and 5% CO_2.

The primary *Il-6*KO fibroblasts were passaged once or twice and used for subsequent experiments. Cells were confirmed to have the classical morphology (long spindle shape) of fibroblasts.

Patients and Skin Samples

This study included two scleroderma patients treated with tocilizumab and three scleroderma patients not treated with tocilizumab. Two scleroderma patients were treated with 8 mg/kg of tocilizumab monthly for 6 months with the permission of the Ethics Committee of Osaka University Hospital and after receipt of informed consent. Detailed patient information was described previously.[15] Skin samples were obtained from patients before and after treatment. Written informed consent was obtained from all patients before skin biopsy.

Immunofluorescent Staining

Wild-type (C57BL/6) and *Il-6*KO fibroblasts were cultured to semiconfluence in 350-mm culture plates. The cultures were fixed in 4% paraformaldehyde at room temperature for 10 minutes and permeabilized with 0.5% Triton in PBS for 5 minutes. The primary Abs used were mouse monoclonal anti-α-smooth muscle actin Ab (1:100, α-SMA; Dako-Cytomation, Carpinteria, CA) , After 1 hour incubation, cells were stained for 30 minutes with Alexa Fluor 488 anti-mouse IgG secondary Ab to α-SMA (Invitrogen, Carlsbad, CA) and Hoechst 33342 (Molecular Probes, Eugene, OR). Mouse IgG_{2a} (Dako-Cytomation, Carpinteria, CA) was used as a control for nonspecific staining.

Paraffin-embedded sections derived from scleroderma patients treated with 6 months of tocilizumab or 6 months of prednisolone, and redundant tissue from surgical specimens were deparaffinized and hydrated. Skin sections derived from patients were brought to a boil in 10 mmol/L sodium citrate buffer (pH 6.0) and then maintained at a subboiling temperature for 10 minutes. After blocking with 5% normal goat serum (Vector Laboratories, Burlingame, CA) in PBST, they were double-stained with mouse monoclonal anti-α-SMA Ab (Dako-Cytomation) and rabbit monoclonal phospho-p44/42 MAPK Ab (Cell Signaling, Beverly, MA). Secondary antibodies were as follows: anti-mouse Alexa Fluor 488 for α-SMA Ab and biotinylated anti-rabbit IgG (Vector Laboratories) plus DyLight594-conjugated Streptavidin (Jackson ImmunoResearch Laboratories, West Grove, PA) for phospho-p44/42 MAPK Ab. Images of immunolabeled sections were captured with a BZ-8000 microscope (Keyence, Osaka, Japan).

Table 1. Effect of MR16-1 on BLM-Induced Dermal Sclerosis in a Prevention Model

	Thickness (mm)			Hardness (Arbitrary)		
	1st (n = 4)	2nd (n = 4)	3rd (n = 4)	1st (n = 4)	2nd (n = 4)	3rd (n = 4)
PBS						
Control Ab	0.137 ± 0.016	0.10 ± 0.01	0.123 ± 0.010	7.09 ± 2.17	6.14 ± 0.72	4.86 ± 1.05
MR16-1	0.11 ± 0.01	0.111 ± 0.011	0.122 ± 0.013	8.91 ± 2.59	6.45 ± 1.49	4.92 ± 0.77
% Change						
Each experiment	81.82	106.33	98.65	125.64	104.91	101.15
Mean ± SE		95.60 ± 7.238			110.6 ± 7.614	
BLM						
Control Ab	0.33 ± 0.04*	0.36 ± 0.05*	0.30 ± 0.07*	24.14 ± 5.58*	16.61 ± 1.90*	9.93 ± 1.51*
MR16-1	0.22 ± 0.03†‡	0.29 ± 0.02‡§	0.16 ± 0.03†	15.47 ± 4.52	8.53 ± 0.80†	5.92 ± 0.49†
% Change						
Each experiment	67.09	81.29	52.22	64.08	51.33	59.59
Mean ± SE		66.89 ± 8.39			58.34 ± 3.74	

(*table continues*)

Values are mean ± SD. To quantify the impact of BLM treatment, % changes were calculated as follows: (evaluative consequences of BLM treatment/that of PBS treatment) × 100 (%).

*$P < 0.01$ PBS+Control Ab versus BLM+Control Ab.

†$P < 0.01$ BLM+Control Ab versus BLM+MR16-1.

‡$P < 0.01$ PBS+MR16-1 versus BLM+MR16-1.

§$P < 0.05$ BLM+Control Ab versus BLM+MR16-1.

HPS, high-power field.

Western Blot Analysis

Wild-type and *Il-6*KO fibroblasts were prepared as described above and cultured to semiconfluence in 100-cm^2 culture plates. Before treatment, fibroblast cultures were washed twice with PBS, and culture media were replaced with low-serum (0.1%fetal bovine serum) Dulbecco's modified Eagle's medium containing 60 IU/mL penicillin, 100 IU/mL streptomycin, and 4 mmol/L glutamine. Low-serum medium was necessary to maintain viability of primary fibroblasts overnight.

Following 12 hours incubation in low-serum medium, treatments were applied to the cultures in fresh low-serum Dulbecco's modified Eagle's medium. Semiconfluent cultures were treated with 10 ng/mL of MR16-1 or 10 μmol/L of PD98058 (Calbiochem, San Diego, CA) for 3 hours, and then 10 ng/mL of recombinant mouse IL-6 (R&D Systems, Minneapolis, MN) was added to the cultures for 24 hours. At indicated time points, culture plates were rinsed twice with ice-cold PBS, and total cell protein was collected in 500 μL of lysis buffer [50 mmol/L Tris-HCl (pH 7.6), 150 mmol/L NaCl, 1% deoxycholic acid, 0.1% sodium dodecyl sulfate, 1% Triton X-100, 1 mmol/L sodium orthovanadate, and protease inhibitor cocktail]. Western blot analysis was performed as previously described.[4] Ten micrograms of protein were fractionated on SDS-polyacrylamide gels and transferred onto PVDF membranes (Bio-Rad, Hercules, CA). Nonspecific protein binding was blocked by incubating the membranes in 5% w/v nonfat milk powder in TBST [50 mmol/L Tris-HCl (pH 7.6), 150 mmol/L NaCl, and 0.1% v/v Tween-20]. The membranes were incubated with mouse monoclonal anti–α-SMA (Dako-Cytomation) Ab at a dilution of 1:1000 overnight at 4°C or with mouse monoclonal anti–β-actin (Sigma-Aldrich) at a dilution of 1:5000 for 30 minutes at room temperature. After three 5-minute washes in TBST, membranes were incubated with horseradish peroxidase–conjugated anti-mouse Ab at a dilution of 1:10,000 for 60 minutes at room temperature. Protein bands were detected using the ECL Plus kit (GE Healthcare, Little Chalfont, UK). Western blot quantification was performed with ImageJ software (NIH, Bethesda, MD) and used to visualize fold expression differences between these treatment groups.

Mice and Induction of Skin Sclerosis

Six-week-old female mice were used in all experiments. C57BL/6 mice were purchased from Japan Clea (Osaka, Japan). Mutant C57BL/6 mice rendered null for IL-6 were described previously[17] and were purchased from the National Institute of Biomedical Innovation (Osaka, Japan). Mice were maintained in our pathogen-free animal facility. All animal care was in accordance with the institutional guidelines of Osaka University. BLM (Nippon Kayaku, Tokyo, Japan) was dissolved in PBS at a concentration of 1 mg/mL and sterilized by filtration. BLM (0.1 mg/100 μL) was injected subcutaneously into the shaved back of the mice daily for 4 weeks with a 27-gauge needle as described by Yamamoto et al.[7] Control mice received 100 μL of PBS instead.

RNA Isolation and Real-Time PCR

Sections of skin lesions and the cutaneous draining lymph nodes (LNs) were removed 1 day after the final injection. Total RNA was isolated using the SV Total RNA Isolation System (Promega, Madison, WI) and reverse transcribed into complementary DNA.

IL-6 expression was measured using the Power SYBR Green PCR Master Mix (Applied Biosystems, Foster City, CA) according to the manufacturer's protocol. Glyceraldehyde-3-phosphate dehydrogenase (GAPDH) was used to normalize the mRNA. Sequence-specific primers were: IL-6, sense 5′-ACACACTGGTTCTGAGGGAC-3′, antisense 5′-TACCACAAGGTTGGCAGGTG-3′; GAPDH,

Table 1. *Continued*

α-SMA–Positive Cells (Cells/HPS)			Mast Cells (Cells/HPS)		
1st (n = 4)	2nd (n = 4)	3rd (n = 4)	1st (n = 4)	2nd (n = 4)	3rd (n = 4)
6.00 ± 4.08	3.50 ± 1.29	8.75 ± 1.50	12.50 ± 4.51	21.67 ± 3.06	31.50 ± 5.45
5.00 ± 1.73	4.00 ± 1.41	10.00 ± 4.16	11.00 ± 1.83	17.33 ± 6.11	29.75 ± 3.50
83.33	114.29	114.29	88.00	80.00	94.44
	104.0 ± 10.32			87.48 ± 4.177	
14.00 ± 1.83*	14.50 ± 4.93*	27.75 ± 0.96*	46.50 ± 8.43*	35.33 ± 5.69*	67.25 ± 5.85*
10.00 ± 1.41	7.00 ± 1.82§	15.25 ± 2.75†	20.25 ± 4.99†	25.00 ± 2.00	29.50 ± 6.19†
71.43	48.28	54.95	43.55	70.75	43.87
	58.22 ± 6.88			52.72 ± 9.02	

Table 2. Effect of MR16-1 on BLM-Induced Dermal Sclerosis in a Treatment Model

	Thickness (mm)		Hardness (arbitrary)		α-SMA–positive cells (cells/HPS)		Mast cells (cells/HPS)	
	1st (n = 4)	2nd (n = 3)	1st (n = 4)	2nd (n = 3)	1st (n = 4)	2nd (n = 3)	1st (n = 4)	2nd (n = 3)
PBS								
Control Ab	0.14 ± 0.02	0.12 ± 0.03	4.80 ± 0.47	6.19 ± 1.29	3.75 ± 1.50	2.33 ± 0.58	13.50 ± 1.73	19.67 ± 2.52
MR16-1	0.12 ± 0.01	0.107 ± 0.006	4.67 ± 0.47	5.68 ± 0.43	3.33 ± 0.56	2.67 ± 1.15	15.33 ± 1.15	21.00 ± 2.00
% Changes	83.64	86.49	97.22	91.78	88.88	106.78	113.58	106.78
BLM								
Control Ab	0.30 ± 0.03*	0.29 ± 0.03*	9.34 ± 1.58*	9.81 ± 1.17†	10.00 ± 2.58*	7.67 ± 0.58*	37.75 ± 2.50*	54.67 ± 8.39*
MR16-1	0.21 ± 0.05‡‖	0.18 ± 0.03§¶	5.46 ± 0.62¶	5.41 ± 0.77¶	5.50 ± 1.29¶	4.00 ± 1.00¶	27.00 ± 2.16§¶	37.00 ± 6.56‡‖
% Changes	70.00	62.50	58.46	55.12	55.00	52.17	71.52	67.68

Mean ± SD is presented. To quantify the impact of MR16-1treatment, % changes were calculated as follows: (evaluative consequences of MR16-1 treatment/that of PBS treatment) × 100 (%).
*P < 0.01 PBS+Control Ab versus BLM+Cont. Ab.
†P < 0.05 PBS+Control Ab versus BLM+Cont. Ab.
‡P < 0.05 BLM+Control Ab versus BLM+MR16-1.
§P < 0.01 PBS+MR16-1 versus BLM+MR16-1.
¶P < 0.01 BLM+Control Ab versus BLM+MR16-1
‖P < 0.05 PBS+MR16-1 versus BLM+MR16-1.
HPS, high-power field.

sense 5′-TGTCATCATACTTGGCAGGTTTCT-3′, antisense 5′-CATGGCCTTCCGTGTTCCTA-3′. Real-time PCR (40 cycles of denaturing at 92°C for 15 seconds and annealing at 60°C for 60 seconds) was run on an ABI 7000 Prism Detection System (Applied Biosystems).

Mouse IL-6 Receptor–Specific Monoclonal Antibody Treatment

Rat anti-mouse IL-6 receptor monoclonal Ab (clone MR16-1, rat $IgG_{1)}$ described previously[18] was provided by Chugai Pharmaceutical (Shizuoka, Japan). Purified rat IgG_1 (isotype-matched control Ab) (Cappel, MP Biomedicals, Solon, OH) was administered as a control. Preventive and therapeutic administration methods are discussed later. Percentage to control values were calculated as follows: (mean actual value/mean control value) × 100.

Enzyme-Linked Immunosorbent Assay of IL-6 Levels in Sera and Conditioned Media

Serum samples were obtained from mice injected with BLM or PBS for 28 days. Conditioned media were obtained from cultured primary dermal fibroblasts of wild-type and *Il-6*KO mice after 24 hours. Serum and conditioned media IL-6 level was measured by enzyme-linked immunosorbent assay using a commercial kit (R&D Systems, Minneapolis, MN) with a detection limit of 7.8 pg/mL.

Vesmeter Measurements

Skin hardness was measured using a Vesmeter.[19] Mice were sacrificed 1 day after the final injection. Skin hardness was measured three times at the injection area, avoiding the backbone of the mouse. Skin hardness was expressed as the area of the depression caused by the

Table 3. Attenuated BLM-Induced Dermal Sclerosis in *Il-6*KO Mice

	Thickness (mm)		Hardness (arbitrary)		α-SMA–positive cells (cells/HPS)		Mast cells (cells/HPS)	
	1st (n = 4)	2nd (n = 3)	1st (n = 4)	2nd (n = 3)	1st (n = 4)	2nd (n = 3)	1st (n = 4)	2nd (n = 3)
WT								
PBS	0.112 ± 0.013	0.14 ± 0.04	4.91 ± 0.38	5.46 ± 0.93	4.75 ± 1.50	8.00 ± 2.00	18.00 ± 3.16	28.33 ± 4.51
BLM	0.32 ± 0.02*	0.29 ± 0.06†	12.38 ± 0.81*	9.69 ± 0.51*	19.75 ± 5.74*	23.33 ± 6.11*	40.25 ± 2.22*	63.33 ± 9.87*
% Change	282.85	203.13	251.99	177.28	415.79	291.67	223.61	223.53
Il-6								
PBS	0.111 ± 0.010	0.12 ± 0.01	5.37 ± 0.48	5.12 ± 0.71	4.00 ± 1.41	6.67 ± 2.52	17.75 ± 2.5	29.5 ± 0.71
BLM	0.22 ± 0.03‡§	0.17 ± 0.03‡	7.14 ± 0.96‡¶	5.85 ± 0.21‡	9.50 ± 4.43‖	13.00 ± 1.73‖	22.75 ± 4.79‡	34.00 ± 7.00‖
% Change	195.71	133.81	132.87	114.21	237.50	195.00	128.17	115.25

Mean ± SD was presented. To quantify the impact of BLM treatment, % changes were calculated as follows: (evaluative consequences of BLM treatment/that of PBS treatment) × 100 (%).
*P < 0.01 WT with PBS versus WT with BLM.
†P < 0.05 WT with PBS versus WT with BLM.
‡P < 0.01 WT with BLM versus *Il-6*KO with BLM.
§P < 0.01 *Il-6*KO with PBS versus *Il-6*KO with BLM.
¶P < 0.05 *Il-6*KO with PBS versus *Il-6*KO with BLM.
‖P < 0.05 WT with BLM versus *Il-6*KO with BLM.
HPS, high-power field; WT, wild-type.

Table 4. Number of Lymph Node Cells in the Scleroderma Mouse Model

	1st experiment (total number/lymph node, × 10^7)			2nd experiment (total number/lymph node, × 10^6)		
	PBS	BLM	% Change	PBS	BLM	% Change
WT						
Control Ab	0.97 ± 0.21 (n = 3)	2.17 ± 0.31* (n = 3)	222.61	1.90 ± 0.41 (n = 4)	3.55 ± 0.21* (n = 4)	186.73
MR16-1	0.76 ± 0.02 (n = 3)	0.80 ± 0.12† (n = 3)	105.29	1.85 ± 0.18 (n = 4)	1.85 ± 0.34† (n = 4)	99.84
*Il-6*KO						
WT	0.81 ± 0.18 (n = 3)	1.53 ± 0.40‡ (n = 3)	190.03	2.36 ± 0.26 (n = 3)	3.71 ± 0.61‡ (n = 3)	157.42
*Il-6*KO	0.66 ± 0.26 (n = 3)	0.54 ± 0.09§ (n = 3)	82.73	1.97 ± 0.67 (n = 3)	2.20 ± 0.29§ (n = 3)	111.51

Mean ± SD was presented. To quantify the impact of BLM treatment, % changes were calculated as follows: (evaluative consequences of BLM treatment/that of PBS treatment) × 100 (%).
*P < 0.01 PBS+Control Ab versus BLM+Cont. Ab.
†P < 0.01 BLM+Control Ab versus BLM+MR16-1.
‡P < 0.05 PBS+Control Ab versus BLM+Cont. Ab.
§P < 0.05 BLM+Control Ab versus BLM+MR16-1.

probe divided by the pressure of the indenter in a connected computer.

Histopathological Analysis

The back skin was removed 1 day after the final injection. Skin pieces were fixed with 10% formaldehyde for 24 hours, embedded in paraffin, and sectioned at 3-μm thickness using a microtome. Sections were stained with hematoxylin and eosin (H&E). Dermal thickness (measured from the epidermal–dermal junction to dermal–fat junction) was determined at ×100 magnification at three randomly selected sites in each animal. Mast cells were identified in 3-μm deparaffinized sections stained with 1% Toluidine Blue, and mast cells were counted in 10 randomly selected sites under × 400 power using light microscopy.

Immunohistochemical Analysis of α-SMA

Sections were cut and processed as described above. For immunohistochemical analysis, sections were deparaffinized by passage through xylene and graded ethanols. Next, endogenous peroxide was blocked using 3% H_2O_2 in methanol for 5 minutes. Slides were blocked with 2% bovine serum albumin for 10 minutes, and stained with primary Ab (anti–α-SMA Ab 1:100 dilution) for 60 minutes. After washing with PBS containing 0.05% Triton, they were developed using Dako ChemMate Envision Kit/horseradish peroxidase (Dako-Cytomation) for 30 minutes, and counterstained with hematoxylin. α-SMA–positive fibroblastic cells were counted in 10 randomly selected sites under × 400 power using light microscopy.

Flow Cytometric Analysis

The skin draining LNs were assessed as a mixture to facilitate analysis. One day after the final infection, mice were sacrificed, and axillary, brachial, and inguinal LNs from each mouse were combined. Cell suspensions of LN cells were stained with antibodies against the following cell surface antigens: CD4, CD8, B220, CD11c, F4/80, and PDCA1 (BD Biosciences, San Jose, CA). Stained cells were analyzed by flow cytometry using a FACSCalibur flow cytometer (BD Biosciences).

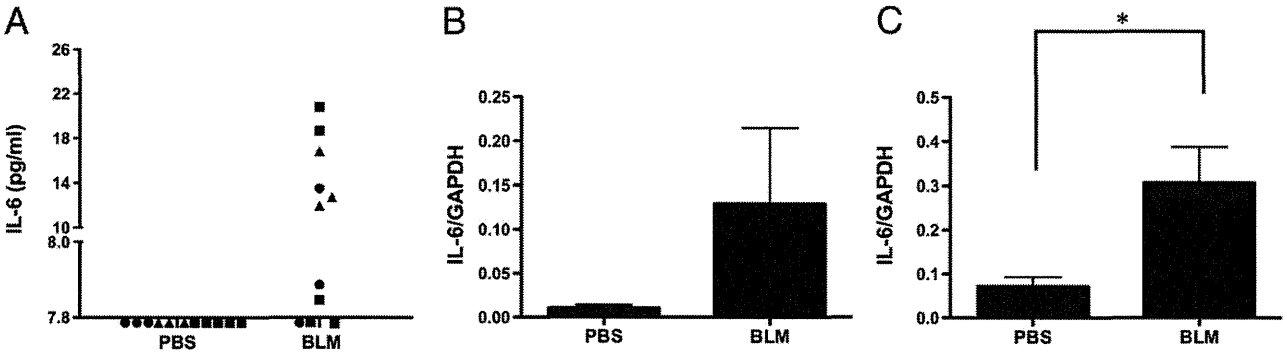

Figure 1. IL-6 production in BLM-treated C57BL/6 mice. C57BL/6 mice treated with PBS or BLM for 4 weeks. **A:** Serum samples were obtained from mice injected with 1 mg/mL BLM (100 μL/day, n = 11) or PBS (100 μL/day, n = 11) for 4 weeks. The data presented are from three experiments of three to five mice each for a total of 11 BLM-treated mice and 11 PBS-treated mice. Serum IL-6 level was measured by enzyme-linked immunosorbent assay using a kit with a detection limit of 7.8 pg/mL (R&D Systems). The mice from different experiments were gave different symbols [box (n = 5), circle (n = 3), and triangles (n = 3)]. Each symbol represents one IL-6 measurement for a single mouse, and symbols below 7.8 pg/mL indicate mice for which IL-6 was below the limit of detection. enzyme-linked immunosorbent assays were run in duplicate for all mice, with similar results. **B** and **C:** Expression of IL-6 mRNA was measured by real-time PCR. RNA was extracted from skin lesions (**B**) and cutaneous draining LNs (**C**) from C57BL/6 mice treated with PBS (n = 3) or BLM (n = 3) for 4 weeks. Data were normalized to the GAPDH internal control. Bars represent mean ± SD. *P < 0.05, unpaired t-test. Data in B and C are from one of two independent experiments that gave similar results. The IL-6/GAPDH data (mean ± SD) for skin lesions (**B**) were as follows: first experiment (n = 3), PBS: 0.011 ± 0.006, BLM: 0.129 ± 0.148 (P = 0.2391); second experiment (n = 3), PBS: 0.142 ± 0.070, BLM: 0.441 ± 0.283 (P = 0.1495). The IL-6/GAPDH data (mean ± SD) for cutaneous draining LNs (**C**) were as follows: first experiment (n = 3), PBS: 0.071 ± 0.038, BLM: 0.306 ± 0.141 (P = 0.0493), second experiment (n = 3), PBS: 0.083 ± 0.0.067, BLM: 0.430 ± 0.175 (P = 0.0321).

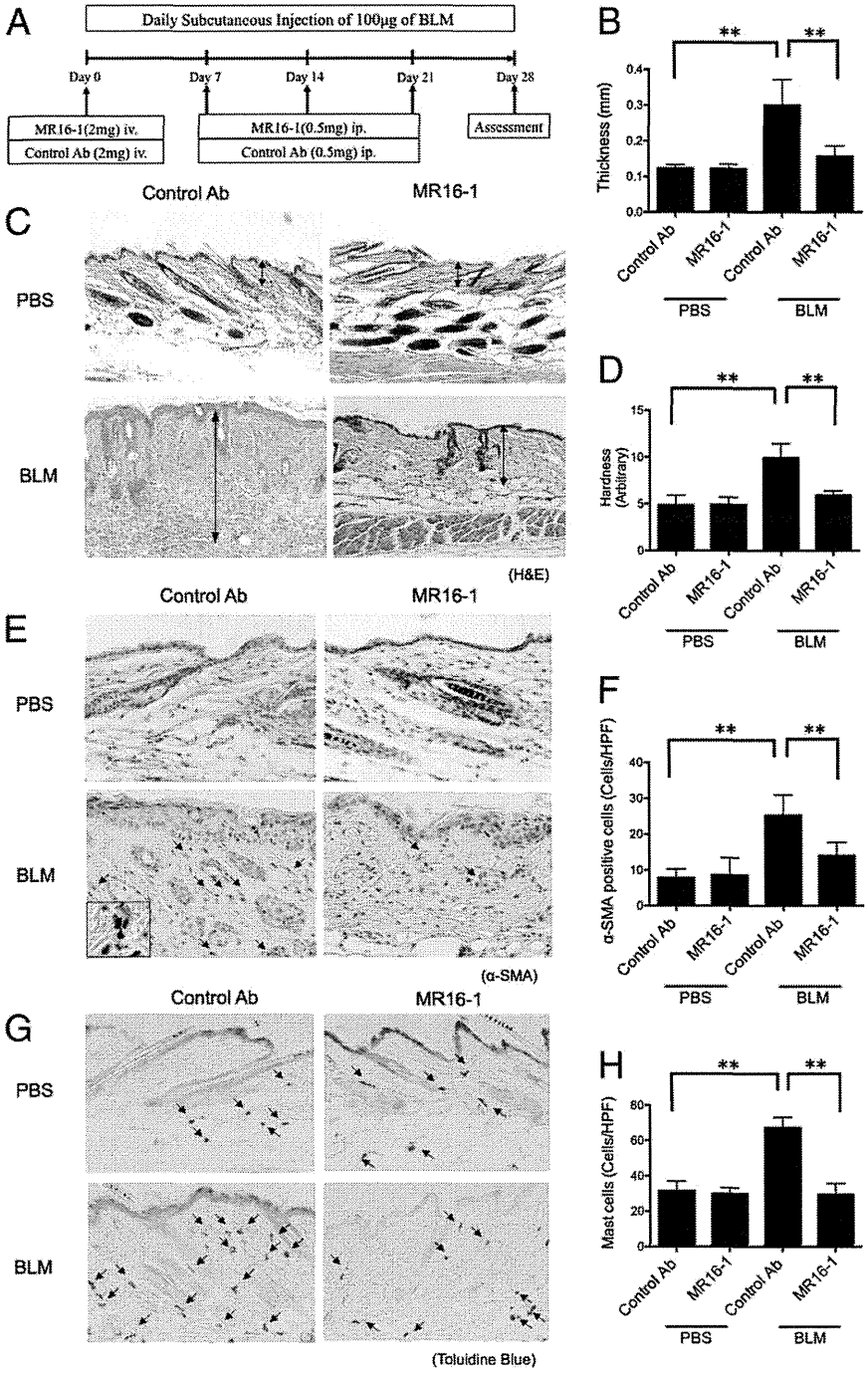

Figure 2. Effect of MR16-1 on BLM-induced dermal sclerosis in a prevention model. **A:** Experimental protocol for prevention of BLM-induced dermal sclerosis by administration of MR16-1 or control Ab to either PBS- or BLM-treated mice ($n = 4$ for each group). Histological and physical examination of the lesional skin was performed on the final day (day 28) of the protocol. **B:** Measurements of dermal thickness ($n = 4$ for each group). **C:** H&E staining of specimens derived from PBS-, or BLM-injected mice treated with MR16-1 or control Ab (original magnification, ×40). The length of each **two-headed arrow** indicates the measurement region of dermal thickness. **D:** Skin hardness measurements obtained using a Vesmeter ($n = 4$ for each group). **E:** Immunohistochemical staining for α-SMA. **Arrows** indicate α-SMA–positive fibroblasts (original magnification, ×100). **Inset** photo shows higher magnification (×200) of α-SMA–positive fibroblasts. **F:** The number of α-SMA–positive fibroblasts per high-power field (HPF, ×400) was determined by observation of 10 random grids. The value graphed is the average of the observation of 10 grids for each of the four mice in the group. **G:** Results of Toluidine Blue staining. **Arrows** indicate the metachromatically stained mast cells (original magnification, ×100). **H:** The number of mast cells per HPF (×400) was determined by observation of 10 random grids. The value graphed is the average of the observation of 10 grids for each of the four mice in the group. **C**, **D**, **F**, and **H:** Bars represent mean ± SD. $^{*}P < 0.05$, $^{**}P < 0.01$, one-way analysis of variance and Bonferroni post hoc multiple comparison. Data presented are from the third of three independent experiments with similar results presented in Table 1.

Computation Methods and Statistical Analysis

All data except change ratios are expressed as mean values ± standard deviations (SDs). To quantify the impact of MR16-1-and BLM treatment, change ratios (%) are calculated for single experiments in Table 1–4. Percent changes in Table 1 are averaged for three experiments and expressed as mean values ± standard errors (SEs). Unpaired *t*-test was used to examine the statistical value between two variable quantities. One-way analysis of variance and the Bonferroni post hoc multiple comparison procedure were used to determine the level of significance between each of three or more variable quantities.

Results

Elevated IL-6 in Mice with BLM-Induced Scleroderma

We first determined the serum concentration and mRNA expression of IL-6 in the skin and cutaneous draining LNs from mice with skin fibrosis induced by subcutaneous

BLM injection. Serum IL-6 levels were undetectable by enzyme-linked immunosorbent assay in all PBS-treated mice, and in 3 of 11 C57BL/6 mice treated with BLM. However, IL-6 was detectable, thus elevated, in 8 of 11 BLM-treated mice (Figure 1A), with a mean of 11.9 ± 5.24 pg/mL (n = 8). IL-6 mRNA expression showed a trend toward increased levels in the skin of mice treated with BLM that was not statistically significant (Figure 1B), and was significantly elevated ($P < 0.05$) in the cutaneous draining LNs of BLM-treated mice relative to PBS-treated mice (Figure 1C). These results are consistent with a role for IL-6 in the pathogenesis of scleroderma in the BLM-induced mouse model.

MR16-1 Prevents BLM-Induced Dermal Sclerosis

We next investigated whether MR16-1, a rat anti-mouse IL-6 receptor monoclonal Ab, could ameliorate the dermal thickening and skin hardening symptoms observed in BLM-treated mice. Figure 2A shows the administration schedule of preventive intervention. Dermal thickness was significantly increased at the BLM injection site of control Ab–treated mice, but nearly normal at the PBS injection site of control Ab–, or MR16-1–treated mice. Importantly, BLM-induced dermal thickening was significantly attenuated by prophylactic administration of MR16-1 (Figure 2, B and C, Table 1).

Skin hardness in the BLM-injected group that was given MR16-1 was also significantly reduced compared to the BLM-injected group that was given the control Ab. The ameliorating effect of MR16-1 on skin hardness was relatively strong compared with the effect on dermal thickness (Figure 2, B and D, Table 1).

To further examine the effects of MR16-1 treatment, the numbers of α-SMA–positive fibroblasts (termed myofibroblasts) (Figure 2, E and F, Table 1) and mast cells (Figure 2, G and H, Table 1), both key players in sclerosis of skin lesions, were evaluated. The numbers of myofibroblasts and mast cells were significantly increased in BLM-injected mice treated with control Ab relative to PBS-injected mice treated with control Ab. In BLM-injected mice treated with MR16-1, the numbers of myofibroblasts and mast cells were decreased significantly compared to the control value (BLM-injected mice treated with control Ab) (Figure 2, E to H, Table 1). These results suggest that treatment with MR16-1 might be effective during the fibrosing phase of scleroderma.

MR16-1 Improves BLM-Induced Dermal Sclerosis

Figure 3A shows the administration schedule of treatment intervention. As expected, the dermal thickness and skin hardness induced by BLM were diminished by therapeutic administration of MR16-1 compared with control Ab (Figure 3, B to D). The numbers of myofibroblasts and mast cells in lesional skin were also decreased by administration of MR16-1 compared with control Ab (Figure 3, E and F). Table 2 summarizes the data from two treatment intervention experiments. These results indicate that IL-6 may contribute to the pathogenesis of BLM-induced scleroderma and that blockade of IL-6 receptor may be a novel treatment of scleroderma.

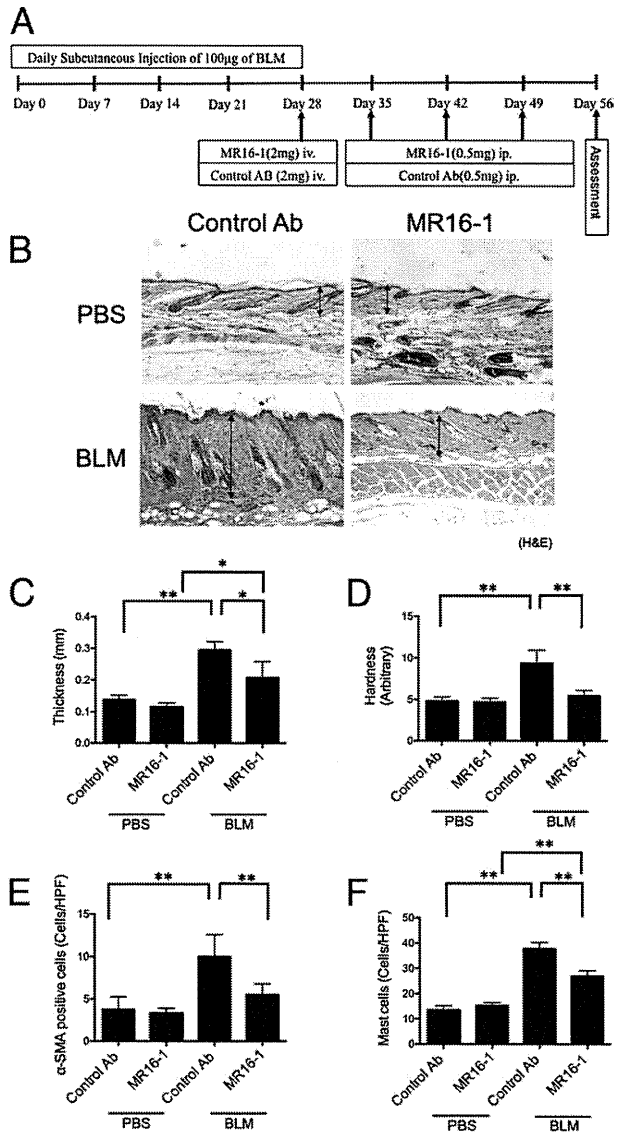

Figure 3. Effect of MR16-1 on BLM-induced dermal sclerosis in a treatment model. **A:** Experimental protocol for treatment of BLM-induced dermal sclerosis by administration of MR16-1 or control Ab to either PBS- or BLM-treated mice (n = 3~4 for each group). The effect of Ab therapy was assessed on day 56. **B:** H&E staining of specimens derived from PBS- or BLM-injected mice treated with MR16-1 or control Ab (original magnification, ×40), and measurements of dermal thickness (**C**) (the measurement region of dermal thickness was indicated with the length of each **two-headed arrow** in **B**) and skin hardness (**D**). The number of α-SMA–positive fibroblasts (**E**) and mast cells (**F**) per HPF (×400) were determined by observation of 10 random grids. The value graphed is the average of the observation of 10 grids for each of the four mice in the group. **C** to **F:** Bars represent mean ± SD. $^{*}P < 0.05$, $^{**}P < 0.01$, one-way analysis of variance and Bonferroni post hoc multiple comparison. Data presented are from the first of two independent experiments with similar results. See Table 2 for data from both experiments.

IL-6 Directly Modulates α-SMA Expression in Dermal Fibroblasts in Vitro

We next focused on whether dermal fibroblasts are a target of IL-6. Nontreated primary dermal fibroblasts from wild-type mice already express α-SMA, and stimulation

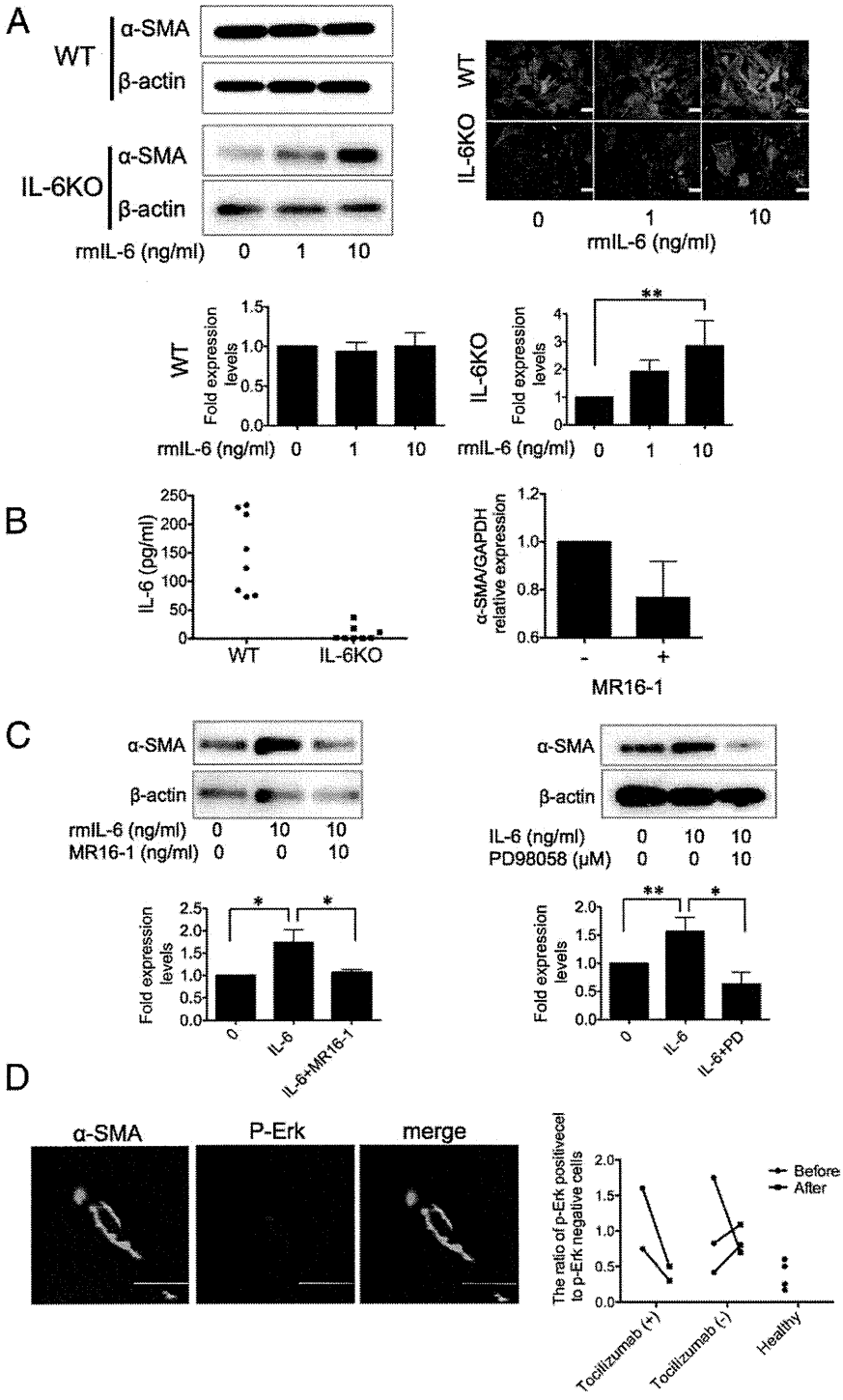

Figure 4. IL-6 induces α-SMA protein expression in cultured *Il-6*KO fibroblasts. **A:** α-SMA expression following recombinant mouse Il-6 (rmIL-6) stimulation was determined by immunofluorescent staining and Western blot analysis. α-SMA and nucleus were show in green and blue, respectively. Scale bar = 100 μm. β-Actin expression was used to determine fold changes in expression by densitometry. Cultured dermal fibroblasts from wild-type (WT) and *Il-6*KO mice were treated with 0, 1, and 10 ng/mL rmIL-6 for 24 hours. These experiments were repeated three times, and the results of densitometric analyses are presented as the fold change (mean ± SD) compared with control. $^{**}P < 0.01$, one-way analysis of variance and Bonferroni post hoc multiple comparisons. **B:** *Il-6* levels in supernatants of cultured dermal fibroblasts from WT and *Il-6*KO mice (**left**) after 24 hours. MR16-1 treatment decreased α-SMA mRNA expression in cultured primary WT dermal fibroblasts (**right**). **C:** MR16-1 and ERK inhibitor, PD98058, attenuated rmIL-6–induced α-SMA protein expression in cultured *Il-6*KO fibroblasts. β-Actin expression was used to determine fold changes in expression by densitometry. These experiments were performed three times, and the results of densitometric analyses are presented as the fold change (mean ± SD) compared with control. $^{**}P < 0.01$, $^{*}P < 0.05$, one-way analysis of variance and Bonferroni post hoc multiple comparisons. **D:** Immunofluorescent staining for phosphorylated ERK (p-ERK, red) and α-SMA (green) in lesional skin derived from two tocilizumab-treated patients with scleroderma. A representative image of p-ERK$^+$, α-SMA$^+$ fibroblasts (original magnification, ×1200) is shown. The number of p-ERK–positive α-SMA–positive fibroblasts per HPF (×400) was determined by observation of 10 random grids. Scale bar = 50 μm. The ratio of p-ERK–positive fibroblasts was calculated as follows: the number of p-ERK$^+$, α-SMA$^+$ fibroblasts/the number of p-ERK$^-$, α-SMA$^+$ fibroblasts.

with exogenous recombinant mouse IL-6 (rmIL-6) did not alter α-SMA expression (Figure 4A). Further, highly expressed levels of endogenous IL-6 from nontreated cultured primary wild-type dermal fibroblasts and decreased levels of α-SMA mRNA expression after MR16 treatment indicated that hyporesponsiveness of cultured primary wild-type dermal fibroblasts to exogenous IL-6 was presumably due to the autocrine regulation of α-SMA by IL-6 (Figure 4B). Thus, we switched to primary *Il-6*KO mouse–derived fibroblasts and evaluated α-SMA expression using immunofluorescent staining and Western blot analysis. Low-level expression was observed in nontreated *Il-6*KO dermal fibroblasts, but stimulation with 1 or 10 ng/mL of rmIL-6 induced α-SMA expression in a dose-dependent manner (Figure 4A). α-SMA induction by rmIL-6 was inhibited by 10 ng/mL MR16-1 and also by the ERK1/2 inhibitor PD98059 (Figure 4C).

These results led us to examine whether the positive effects of clinical treatment with tocilizumab might correlate with reduced numbers of ERK-activated α-SMA–pos-

itive dermal fibroblasts in lesional skin of scleroderma patients. The number of Erk-activated α-SMA–positive cells in lesional skin in scleroderma patients treated with tocilizumab for 6 months was reduced to a similar level as in healthy skin, whereas the number in scleroderma patients treated with 10 mg/day of prednisolone for 6 months without tocilizumab was diminished in one patient and increased in two patients (Figure 4D).

Attenuated BLM-Induces Dermal Sclerosis in Il-6KO Mice

To investigate the role of IL-6 in BLM-induced dermal sclerosis, *Il-6*KO mice received subcutaneous injection of BLM or PBS for 4 weeks, and histological and physical examination of the lesional skin was performed (Figure 5A, Table 3). We found that BLM-induced dermal sclerosis in *Il-6*KO mice was attenuated compared with that in wild-type mice. Lack of visible changes in the skin between PBS-treated *Il-6*KO mice and PBS-treated wild-type mice indicated that IL-6 might not be involved in dermal homeostasis (Figure 5A). After 4 weeks of BLM treatment, dermal thickness and skin hardness in *Il-6*KO mice were significantly attenuated compared to wild-type mice (Figure 5A). The numbers of α-SMA–positive cells and mast cells in BLM-treated *Il-6*KO mice were significantly reduced compared to BLM-treated wild-type mice (Figure 5B). Table 3 summarizes the data from two experiments. These results indicate that IL-6 is likely to play an important role in promoting the fibrogenic responses elicited by BLM treatment.

Enlarged Draining LNs Are Reduced in Size by a Block of IL-6 in the Mouse Model and in a Patient with Scleroderma

We found that cutaneous draining LNs were visibly enlarged by BLM treatment in the scleroderma model mice, but not by PBS treatment (Figure 6A, Table 4). The total LN cell count per LN in control Ab–treated BLM-injected mice was significantly increased compared with control Ab–treated PBS-injected mice, and decreased by administration of MR16-1 to BLM-injected mice. Although it was only from a single experiment with a small number of mice, the weight per LN also showed similar findings to the results of the total LN cell count per LN. However, no histological differences were observed between LNs from BLM- and PBS-injected control Ab–treated mice (Figure 6A). Detailed cell fractionation analysis (using cell-surface antigens CD4, CD8, B220, CD11c, F4/80, and PDCA1) of cells isolated from the draining LNs revealed that the ratio of $PDCA1^{+}CD11c^{+}$ double-positive cells [plasmacytoid dendritic cells (pDCs)] was significantly increased in the draining LNs of prophylactically MR16-1–treated model mice (Figure 6B). Further, draining LNs were not grossly enlarged in BLM-treated *Il-6*KO mice (Figure 6C, Table 4), consistent with weight and total cell count per LN measurements in the normal range (Figure 6C).

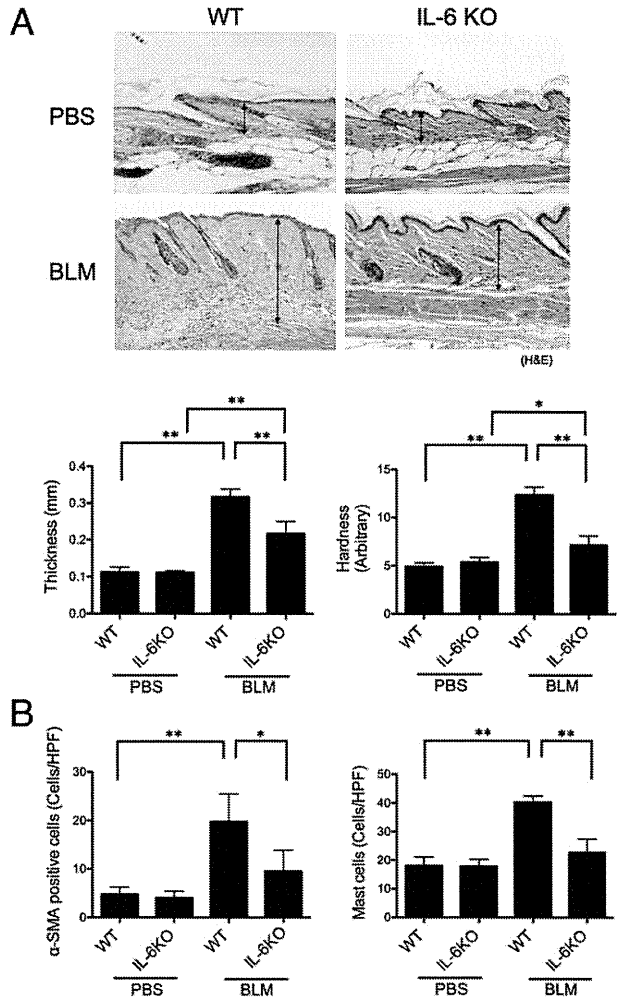

Figure 5. Attenuated BLM-induced dermal sclerosis in *Il-6*KO mice. **A:** H&E staining of skin specimen derived from PBS- and BLM-treated wild-type (WT) and *Il-6*KO mice (original magnification × 40), and measurements of dermal thickness (**lower left panel**) and skin hardness (**lower right panel**). The length of the **two-headed arrows** indicates the measurement region of dermal thickness. **B:** The number of α-SMA–positive fibroblasts (**left panel**) and mast cells (**right panel**) per HPF (×400) was determined by observation of 10 random grids. **A** and **B:** Bars represent mean ± SD ($n = 4$ for each group). $^{*}P < 0.05$, $^{**}P < 0.01$, one-way analysis of variance and Bonferroni post hoc multiple comparison. Data presented are from the first of two independent experiments that yielded similar results, and Table 3 presents data from both experiments.

We then examined whether LNs were enlarged in a patient with scleroderma, and found swelling of axillary LNs on computed tomography scan (Figure 6D), which was not detected after the administration of tocilizumab (Figure 6D).

Discussion

Our study demonstrates the critical role of IL-6 in dermal sclerosis. Blockade of IL-6 receptor with MR16-1 in the BLM-treated mice alleviates dermal sclerosis. This report also addresses outstanding problems in scleroderma pathogenesis, including the target of IL-6.

The source(s) of the elevated IL-6 in the sera of patients with scleroderma are still unclear. Several lines of

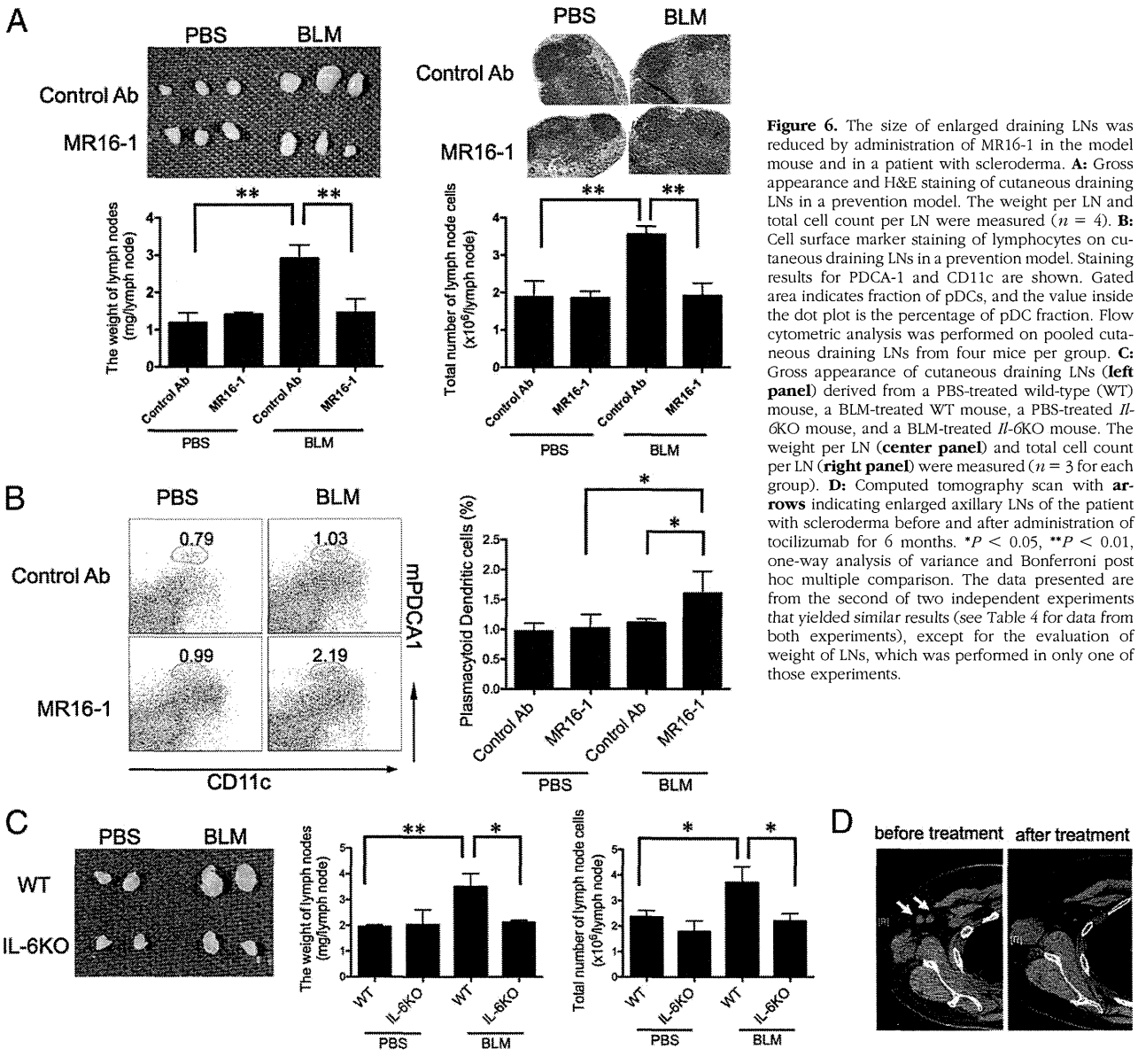

Figure 6. The size of enlarged draining LNs was reduced by administration of MR16-1 in the model mouse and in a patient with scleroderma. **A:** Gross appearance and H&E staining of cutaneous draining LNs in a prevention model. The weight per LN and total cell count per LN were measured ($n = 4$). **B:** Cell surface marker staining of lymphocytes on cutaneous draining LNs in a prevention model. Staining results for PDCA-1 and CD11c are shown. Gated area indicates fraction of pDCs, and the value inside the dot plot is the percentage of pDC fraction. Flow cytometric analysis was performed on pooled cutaneous draining LNs from four mice per group. **C:** Gross appearance of cutaneous draining LNs (**left panel**) derived from a PBS-treated wild-type (WT) mouse, a BLM-treated WT mouse, a PBS-treated *Il-6*KO mouse, and a BLM-treated *Il-6*KO mouse. The weight per LN (**center panel**) and total cell count per LN (**right panel**) were measured ($n = 3$ for each group). **D:** Computed tomography scan with **arrows** indicating enlarged axillary LNs of the patient with scleroderma before and after administration of tocilizumab for 6 months. $^{*}P < 0.05$, $^{**}P < 0.01$, one-way analysis of variance and Bonferroni post hoc multiple comparison. The data presented are from the second of two independent experiments that yielded similar results (see Table 4 for data from both experiments), except for the evaluation of weight of LNs, which was performed in only one of those experiments.

evidence suggest peripheral blood mononuclear cells are a source. The supernatant concentration of IL-6 was reported to be statistically significantly elevated in peripheral blood mononuclear cells[6,20,21] and in T-cell lines[6] derived from patients with systemic sclerosis compared with healthy controls. It also has been reported that experimentally activated B cells might be prone to produce IL-6.[22,23] Other lines of evidence implicate dermal fibroblasts as an important source of IL-6.[13,24–28] In this report, although the expression of IL-6 mRNA in both lesional skin and draining LNs was increased by BLM treatment, the specific cell type producing IL-6 was not identified. Further studies are required to clarify the source(s) of IL-6.

How does secreted IL-6 contribute to the pathogenesis of scleroderma? IL-6 might modulate α-SMA expression in dermal fibroblasts and induce myofibroblasts, which are known to produce collagen[29] and induce sclerotic change.[11,30] We observed IL-6 effects on α-SMA expression from *Il-6*KO dermal fibroblasts *in vitro* in this study (Figure 4A). Unexpectedly, nontreated cultured wild-type dermal fibroblasts strongly expressed α-SMA (Figure 4A), the expression of which was not affected by exogenous IL-6, whereas MR16-1 treatment decreased the expression of α-SMA mRNA (Figure 4, A and B). Therefore, continuous autocrine production of IL-6 by wild-type cultured dermal fibroblasts might increase the threshold for reactivity to IL-6.

Furthermore, in both prevention and treatment protocols with MR16-1, the reduction in dermal sclerosis was accompanied by decreasing numbers of myofibroblasts, which are known as activated fibroblasts with strong fibrogenic property. The absence of myofibroblasts at the BLM injection site of *Il-6*KO mice indicates that IL-6–induced dermal sclerosis occurs via induction of myofibroblasts. Thus, we hypothesize that MR16-1 and tocilizumab have favorable effects on scleroderma via prevention of fibroblast activation. Administration of tocili-

zumab to scleroderma patients exhibited ameliorating effects of skin sclerosis,[15] and seemed to reduce the number of Erk-activated α-SMA–positive fibroblast in lesional skin (Figure 4D). These findings were inconclusive because of the number of cases, and further studies were required.

Another finding was reduction of LN swelling by MR16-1 treatment in mice in the BLM-induced model of scleroderma. We could not determine whether the LN swelling associated with BLM treatment was a cause or effect of BLM-induced skin sclerosis. Examination of the differential ratios of leukocytes, such as T cells, B cells, and macrophages, did not give any insight, as these were not altered after 4 weeks of BLM injection (data not shown). However, there was a slight, but significant, increase in the numbers of cells double-positive for PDCA-1^+CD11c^+ (Figure 6D) or $B220^+CD11c^+$ (data not shown) in the draining LNs of MR16-1–treated mice relative to control Ab–treated mice in the prevention model. This suggests that IL-6 might affect pDC numbers in the LNs. LN swelling is not a well-known symptom in scleroderma, and only a few articles describe LN findings in scleroderma.[31] We should keep an eye on such symptoms.

Recent studies have indicated that pDCs may promote scleroderma via secretion of type 1 interferon,[32] and induction of type 1 interferon was found by anti-topoisomerase antibody-containing serum, but not by anti-centromere antibody.[32,33] However, other data suggest MHC class II–restricted antigen presentation by pDCs might inhibit T-cell–mediated autoimmunity via selective expansion of Ag-specific natural regulatory T cells.[34] Because MHC class II–restricted proliferation of $CD4^+$ T cells had been previously thought to contribute to the pathogenesis of scleroderma,[35] one could speculate that an increased ratio of pDCs might prevent skin sclerosis via regulating peripheral tolerance. However, it is clear that the function of pDCs in pathogenesis of scleroderma is complex and needs further study.

The clear positive effects of IL-6 inhibition in mouse models with scleroderma indicate that further study of IL-6–secreting cells, effectors, and signaling in scleroderma holds great promise for the development of therapies for scleroderma, as well as for other diseases in which IL-6 can play a pivotal role.

Acknowledgments

We thank Prof. Junji Takeda (Osaka University) for expert comments and Dr. Toshiaki Hanafusa, Kenjyu Nishida, and Han Fu for technical assistance.

References

1. Preliminary criteria for the classification of systemic sclerosis (scleroderma). Subcommittee for scleroderma criteria of the American Rheumatism Association Diagnostic and Therapeutic Criteria Committee. Arthritis Rheum 1980, 23:581–590
2. Needleman BW, Wigley FM, Stair RW: Interleukin-1, interleukin-2, interleukin-4, interleukin-6, tumor necrosis factor alpha, and interferon-gamma levels in sera from patients with scleroderma. Arthritis Rheum 1992, 35:67–72
3. Hebbar M, Gillot JM, Hachulla E, Lassalle P, Hatron PY, Devulder B, Janin A: Early expression of E-selectin, tumor necrosis factor alpha, and mast cell infiltration in the salivary glands of patients with systemic sclerosis. Arthritis Rheum 1996, 39:1161–1165
4. Terao M, Murota H, Kitaba S, Katayama I: Tumor necrosis factor-alpha processing inhibitor-1 inhibits skin fibrosis in a bleomycin-induced murine model of scleroderma. Exp Dermatol 2009, 19:38–43
5. Murota H, Hamasaki Y, Nakashima T, Yamamoto K, Katayama I, Matsuyama T: Disruption of tumor necrosis factor receptor p55 impairs collagen turnover in experimentally induced sclerodermic skin fibroblasts. Arthritis Rheum 2003, 48:1117–1125
6. Scala E, Pallotta S, Frezzolini A, Abeni D, Barbieri C, Sampogna F, De Pita O, Puddu P, Paganelli R, Russo G: Cytokine and chemokine levels in systemic sclerosis: relationship with cutaneous and internal organ involvement. Clin Exp Immunol 2004, 138:540–546
7. Yamamoto T, Takagawa S, Katayama I, Yamazaki K, Hamazaki Y, Shinkai H, Nishioka K: Animal model of sclerotic skin. I: local injections of bleomycin induce sclerotic skin mimicking scleroderma, J Invest Dermatol 1999, 112:456–462
8. Yamamoto T, Takagawa S, Katayama I, Nishioka K: Anti-sclerotic effect of transforming growth factor-beta antibody in a mouse model of bleomycin-induced scleroderma. Clin Immunol 1999, 92:6–13
9. Kuwana M, Medsger TA Jr., Wright TM: Analysis of soluble and cell surface factors regulating anti-DNA topoisomerase I autoantibody production demonstrates synergy between Th1 and Th2 autoreactive T cells. J Immunol 2000, 164:6138–6146
10. Kishimoto T: The biology of interleukin-6. Blood 1989, 74:1–10
11. Gallucci RM, Lee EG, Tomasek JJ: IL-6 modulates alpha-smooth muscle actin expression in dermal fibroblasts from IL-6-deficient mice. J Invest Dermatol 2006, 126:561–568
12. Duncan MR, Berman B: Stimulation of collagen and glycosaminoglycan production in cultured human adult dermal fibroblasts by recombinant human interleukin 6. J Invest Dermatol 1991, 97:686–692
13. Kawaguchi Y, Hara M, Wright TM: Endogenous IL-1alpha from systemic sclerosis fibroblasts induces IL-6 and PDGF-A. J Clin Invest 1999, 103:1253–1260
14. Nishimoto N, Kishimoto T: Interleukin 6: from bench to bedside. Nat Clin Pract Rheumatol 2006, 2:619–626
15. Shima Y, Kuwahara Y, Murota H, Kawai M, Hirano T, Arimitsu J. Narazaki M, Hagihara K, Ogata A, Katayama I, Kawase I, Kishimoto T, Tanaka T: The skin of patients with systemic sclerosis softened during the treatment with anti-IL-6 receptor antibody tocilizumab. Rheumatology 2010, 49:2408–12
16. Gallucci RM, Sloan DK, Heck JM, Murray AR, O'Dell SJ: Interleukin 6 indirectly induces keratinocyte migration. J Invest Dermatol 2004, 122:764–772
17. Kopf M, Baumann H, Freer G, Freudenberg M, Lamers M, Kishimoto T, Zinkernagel R, Bluethmann H, Kohler G: Impaired immune and acute-phase responses in interleukin-6-deficient mice. Nature 1994, 368:339–342
18. Takagi N, Mihara M, Moriya Y, Nishimoto N, Yoshizaki K, Kishimoto T, Takeda Y, Ohsugi Y: Blockage of interleukin-6 receptor ameliorates joint disease in murine collagen-induced arthritis. Arthritis Rheum 1998, 41:2117–2121
19. Kuwahara Y, Shima Y, Shirayama D, Kawai M, Hagihara K, Hirano T, Arimitsu J, Ogata A, Tanaka T, Kawase I: Quantification of hardness, elasticity and viscosity of the skin of patients with systemic sclerosis using a novel sensing device (Vesmeter): a proposal for a new outcome measurement procedure. Rheumatology (Oxford) 2008, 47: 1018–1024
20. Hasegawa M, Sato S, Ihn H, Takehara K: Enhanced production of interleukin-6 (IL-6), oncostatin M and soluble IL-6 receptor by cultured peripheral blood mononuclear cells from patients with systemic sclerosis. Rheumatology (Oxford) 1999, 38:612–617
21. Crestani B, Seta N, De Bandt M, Soler P, Rolland C, Dehoux M, Boutten A, Dombret MC, Palazzo E, Kahn MF, et al.: Interleukin 6 secretion by monocytes and alveolar macrophages in systemic sclerosis with lung involvement. Am J Respir Crit Care Med 1994, 149: 1260–1265
22. Saito E, Fujimoto M, Hasegawa M, Komura K, Hamaguchi Y, Kaburagi Y, Nagaoka T, Takehara K, Tedder TF, Sato S: CD19-dependent B lymphocyte signaling thresholds influence skin fibrosis and

autoimmunity in the tight-skin mouse. J Clin Invest 2002, 109:1453–1462
23. Matsushita T, Hasegawa M, Yanaba K, Kodera M, Takehara K, Sato S: Elevated serum BAFF levels in patients with systemic sclerosis: enhanced BAFF signaling in systemic sclerosis B lymphocytes. Arthritis Rheum 2006, 54:192–201
24. Takemura H, Suzuki H, Fujisawa H, Yuhara T, Akama T, Yamane K, Kashiwagi H: Enhanced interleukin 6 production by cultured fibroblasts from patients with systemic sclerosis in response to platelet derived growth factor. J Rheumatol 1998, 25:1534–1539
25. Kawaguchi Y, Nishimagi E, Tochimoto A, Kawamoto M, Katsumata Y, Soejima M, Kanno T, Kamatani N, Hara M: Intracellular IL-1alpha-binding proteins contribute to biological functions of endogenous IL-1alpha in systemic sclerosis fibroblasts, Proc Natl Acad Sci U S A 2006, 103:14501–14506
26. Fukasawa C, Kawaguchi Y, Harigai M, Sugiura T, Takagi K, Kawamoto M, Hara M, Kamatani N: Increased CD40 expression in skin fibroblasts from patients with systemic sclerosis (SSc): role of CD40-CD154 in the phenotype of SSc fibroblasts. Eur J Immunol 2003, 33:2792–2800
27. Kadono T, Kikuchi K, Ihn H, Takehara K, Tamaki K: Increased production of interleukin 6 and interleukin 8 in scleroderma fibroblasts. J Rheumatol 1998, 25:296–301
28. Koch AE, Kronfeld-Harrington LB, Szekanecz Z, Cho MM, Haines GK, Harlow LA, Strieter RM, Kunkel SL, Massa MC, Barr WG, Jimenez SA: In situ expression of cytokines and cellular adhesion molecules in the skin of patients with systemic sclerosis. Their role in early and late disease. Pathobiology 1993, 61:239–246
29. Wynn TA: Cellular and molecular mechanisms of fibrosis. J Pathol 2008, 214:199–210
30. Kirk TZ, Mark ME, Chua CC, Chua BH, Mayes MD: Myofibroblasts from scleroderma skin synthesize elevated levels of collagen and tissue inhibitor of metalloproteinase (TIMP-1) with two forms of TIMP-1. J Biol Chem 1995, 270:3423–3428
31. Ofstad E: Scleroderma (progressive systemic sclerosis). A case involving polyneuritis and swelling of the lymph nodes. Acta Rheumatol Scand 1960, 6:65–75
32. Eloranta ML, Franck-Larsson K, Lovgren T, Kalamajski S, Ronnblom A, Rubin K, Alm GV, Ronnblom L: Type I interferon system activation and association with disease manifestations in systemic sclerosis. Ann Rheum Dis 2010, 69:1396–1402
33. Kim D, Peck A, Santer D, Patole P, Schwartz SM, Molitor JA, Arnett FC, Elkon KB: Induction of interferon-alpha by scleroderma sera containing autoantibodies to topoisomerase I: association of higher interferon-alpha activity with lung fibrosis. Arthritis Rheum 2008, 58: 2163–2173
34. Irla M, Kupfer N, Suter T, Lissilaa R, Benkhoucha M, Skupsky J, Lalive PH, Fontana A, Reith W, Hugues S: MHC class II-restricted antigen presentation by plasmacytoid dendritic cells inhibits T cell-mediated autoimmunity. J Exp Med 2010, 207:1891–1905
35. Kuwana M, Medsger TA Jr., Wright TM: T cell proliferative response induced by DNA topoisomerase I in patients with systemic sclerosis and healthy donors. J Clin Invest 1995, 96:586–596

Pigment Cell Melanoma Res. **25**; 219–230

ORIGINAL ARTICLE

Dysregulation of melanocyte function by Th17-related cytokines: significance of Th17 cell infiltration in autoimmune vitiligo vulgaris

Yorihisa Kotobuki[1,2,*], Atsushi Tanemura[1,*], Lingli Yang[1,2], Saori Itoi[1], Mari Wataya-Kaneda[1], Hiroyuki Murota[1], Minoru Fujimoto[2], Satoshi Serada[2], Tetsuji Naka[2] and Ichiro Katayama[1]

1 Department of Dermatology Integrated Medicine, Osaka University Graduate School of Medicine, Osaka, Japan **2** Laboratory for Immune Signal, National Institute of Biomedical Innovation

CORRESPONDENCE Atsushi Tanemura, e-mail: tanemura@derma.med.osaka-u.ac.jp
*These authors contributed equally to this work.

KEYWORDS vitiligo/Th17 cell/Th17-related cytokines/melanocyte/interaction with skin-resident cells

PUBLICATION DATA Received 19 July 2011, revised and accepted for publication 30 November 2011, published online 3 December 2011

doi: 10.1111/j.1755-148X.2011.00945.x

Summary

The aim of this study was to determine whether CD4$^+$IL-17A$^+$Th17 cells infiltrate vitiligo skin and to investigate whether the proinflammatory cytokines related to Th17 cell influence melanocyte enzymatic activity and cell fate. An immunohistochemical analysis showed Th17 cell infiltration in 21 of 23 vitiligo skin samples in addition to CD8$^+$ cells on the reticular dermis. An in vitro analysis showed that the expression of MITF and downstream genes was downregulated in melanocytes by treatment with interleukin (IL)-17A, IL-1β, IL-6, and tumor necrosis factor (TNF)-α. Treatment with these cytokines also induced morphological shrinking in melanocytes, resulting in decreased melanin production. In terms of local cytokine network in the skin, IL-17A dramatically induced IL-1β, IL-6, and TNF-α production in skin-resident cells such as keratinocytes and fibroblasts. Our results provide evidence of the influence of a complex Th17 cell-related cytokine environment in local depigmentation in addition to CD8$^+$ cell-mediated melanocyte destruction in autoimmune vitiligo.

Introduction

In the epidermis, the epidermal melanin unit is reliant on the close interaction between a melanocyte and the associated pool of keratinocytes, and several inflammatory cytokines affect melanocyte migration, proliferation, and differentiation. Therefore, the local skin microenvironment generated by the skin-resident cells may be considered a crucial milieu for the normal life and functions of epidermal melanocytes (Chalraborty and Pawelek, 1993).

Vitiligo, a representative depigmented skin disorder associated with melanocyte destruction, affects an estimated 1% of the world's population (Howitz et al., 1977). Although the cellular immunoresponse, mainly of CD8$^+$ cytotoxic T cells, to the melanocyte-specific proteins MART-1, tyrosinase (TYR), and TRPs-1 and -2 has been shown to destroy functional melanocytes in

Significance

Here we show that not only cytotoxic T cells, which have been thought to play a major role in autoimmune vitiligo, but also infiltration of Th17 cells may play a role in vitiligo skin. In fact, we find that in vitro, a network of Th17 cell-related cytokines directly affect melanocyte activity and function, including downregulation of melanin production and shrinkage of melanocytes. These observations may shed light on the functional significance of TH17 cells in autoimmune vitiligo.

autoimmune vitiligo, this does not provide a full explanation for the etiology of vitiligo (Norris et al., 1994; Ogg et al., 1998; Okamoto et al., 1998; Ongenae et al., 2003). In addition to the autoimmune mechanism, recent reports have shown that there is a significant increase in the expression of inflammatory cytokines in affected skin compared with unaffected skin, and several investigators have proposed that the influence of local cytokines may be related to the induction and maintenance of vitiligo (Basak et al., 2009; Moretti et al., 2002, 2009; Ratsep et al., 2008). Although the representative cytokines increased in vitiligo skin have been reported to include interleukin (IL)-2, tumor necrosis factor (TNF)-α, and interferon (IFN)-γ (Caixia et al., 1999), there is no direct evidence of their function in the melanocyte destruction observed in vitiligo.

Upon induction by transforming growth factor (TGF)-b and IL-6, a subset of $CD4^+$ helper T cells develops as Th17 cells (Diveu et al., 2008). IL-17A is a cystine-linked homodimeric proinflammatory cytokine produced by Th17 cells, which form a distinct subset of the $CD4^+$ T-cell lineage. IL-17A stimulates the production of IL-1β, TNF-α, and IL-6 (Kolls and Linden, 2004; Liang et al., 2006). In the past decade, Th17 cells have been identified in autoimmune skin inflammatory disorders such as psoriasis and atopic dermatitis (Asarch et al., 2008; Fitch et al., 2009). A recent study showed a positive correlation between serum IL-17 levels and the extent of the depigmentation patch area in vitiligo, thus suggesting that Th17 cells, rather than regulatory T cells, are involved in vitiligo (Basak et al., 2009). Another study demonstrated elevated IL-17 levels in lesional skin and serum of patients with vitiligo compared with those of controls (Bassiouny and Shaker, 2011). These results indicated the importance of the secreted cytokine environment surrounding vitiliginous melanocytes in terms of vitligo etiology. In the present study, we investigated whether Th17 cells infiltrate vitiligo skin as in cases of psoriasis and whether the proinflammatory cytokines produced by Th17 cells, keratinocytes, and fibroblasts are altered in vitiligous lesions in a series of non-segmental vitiligo patients. The Th17-related cytokines tested included IL-17A and IL-22, in addition to IL-1β and IL-6, which have been reported to inhibit melanocyte activity (Kamaraju et al., 2002; Kholmanskikh et al., 2010).

MITF-M (microphthalmia-associated transcription factor-M) is a master transcription factor regulating melanocyte fate and melanogenic activity; it is distinctly expressed in melanocytes and mast cells (Levy et al., 2006). MITF expression and phosphorylation are important for the regulation of melanogenesis and melanocyte survival because the target genes of MITF encode the apoptosis regulator protein, B-cell lymphoma 2 (Bcl-2), in addition to melanogenic enzymes, tyrosinase, tyrosinase-related protein-1 (TRP-1), and dopachrome tautomerase (DCT), which are indispensable for maintaining melanocyte function (Levy et al., 2006). Because of the reduction in active melanocytes expressing these proteins in the vitiligo epidermis, the dysregulation of MITF expression has to be resolved to effectively treat vitiligo. In addition, the mRNA levels of *MITF* and *BCL2* were decreased in the lesional skin compared with the non-lesional skin of vitiligo patients (Kingo et al., 2008). The expression levels of IL-6 and TNF-α were also significantly higher in the lesional skin, indicating that in vitiligo lesions, there is increased expression of cytokines that are paracrine inhibitors of melanocytes (Moretti et al., 2002, 2009). These cytokines are produced mainly by keratinocytes, so it is possible that these cells may be abnormal in vitiligo. In addition, the expression of cytokines was unchanged in healthy skin compared with non-lesional skin, suggesting that the change observed in vitiligo lesional skin is possibly related to, or contributes to, depigmentation. Therefore, it is conceivable that there is a previously unrecognized mechanism involved in the regulation of the pigmentation-hypopigmentation balance in addition to a cytotoxic effect by $CD8^+$ T cell.

In this study, we examined the direct effect of Th17-related cytokines on MITF expression to determine the effects on the resulting cytokine involvement on the regulation of critical melanocyte behavior. We discuss the significance of Th17 cell infiltration in autoimmune vitiligo skin and propose a functional involvement of Th17 cell-related proinflammatory cytokines in vitiligo.

Results

Vitiligo skin develops in association with Th17 cell infiltration

Approval for this study was obtained from the Institutional Review Board of the Osaka University Hospital. To investigate whether Th17 cells infiltrate vitiligo skin, we performed immunostaining for IL-17A and CD4 using specific antibodies. Th17 cells were defined as the cells expressing both markers after exclusion of gamma delta T cells. Twenty-three vitiligo patients were enrolled in this study (see Table 1 for details) and were divided into 17 generalized, four localized, and two seg-

Table 1. Patients' characteristics and the infiltration status of Th17 cells

Age	27–81			
Gender				
Female	13			
Male	10			
Disease duration (yr)	0.1–26			
Mean	6.2			
	(n)	>50/field	<50/field	Not detected
Th17 cell infiltration				
Generalized type	17	11	6	0
Segmental type	4	2	0	2
Localized type	2	2	0	0
Total	23	15	6	2

mental types. The ages of the enrolled patients ranged from 27 to 81 yr, and the subjects included 13 women and 10 men. As a representative case, we show a 79-yr-old man who had experienced enlarging symmetrical depigmented macules on the whole body including face starting 2 yr previously who was positive for antithyroid antibody in the blood test (Figure 1).

Biopsy specimens were obtained from the leading edge of lesional skin on the left upper arm and were processed for the designated immunostaining. The immunohistochemical analysis revealed significant infiltration of IL-17A$^+$CD4$^+$ cells, that is, Th17 cells, mainly on the reticular dermis and perivascular region (Figure 1A). IL-17A expression was confirmed by RT-PCR using vitiligo tissue RNA. Psoriasis skin, a representative skin disease with Th17 cell infiltration, was loaded as a positive control for RT-PCR (Figure 1A). CD8$^+$ T cells were also observed, mainly below the epidermis, whereas Foxp3$^+$ cells and CD20$^+$ B cells had only faintly infiltrated (Figure 1B). Melan-A positive melanocytes were not observed in the vitiligo epidermis with inflammatory cell infiltration, whereas they were frequently located in the non-lesional skin (Figure 1B lower right panel and Inbox, respectively).

We observed a significant number of Th17 cells in 21 of 23 of the patient skin samples, and more than 50 double-positive cells per high power field were observed in 15 patients, while there was sparse infiltration in normal skin. Th17 cells were not detected in the two cases of localized type. Psoriatic skin was used as a positive control for this staining and showed the involvement as dense infiltration through the epidermis and upper dermis of pathogenic inflammatory cells whose localization was different from that in vitiligo (Figure 1C). Although we suspected that early onset and generalized type vitiligo had more opportu-

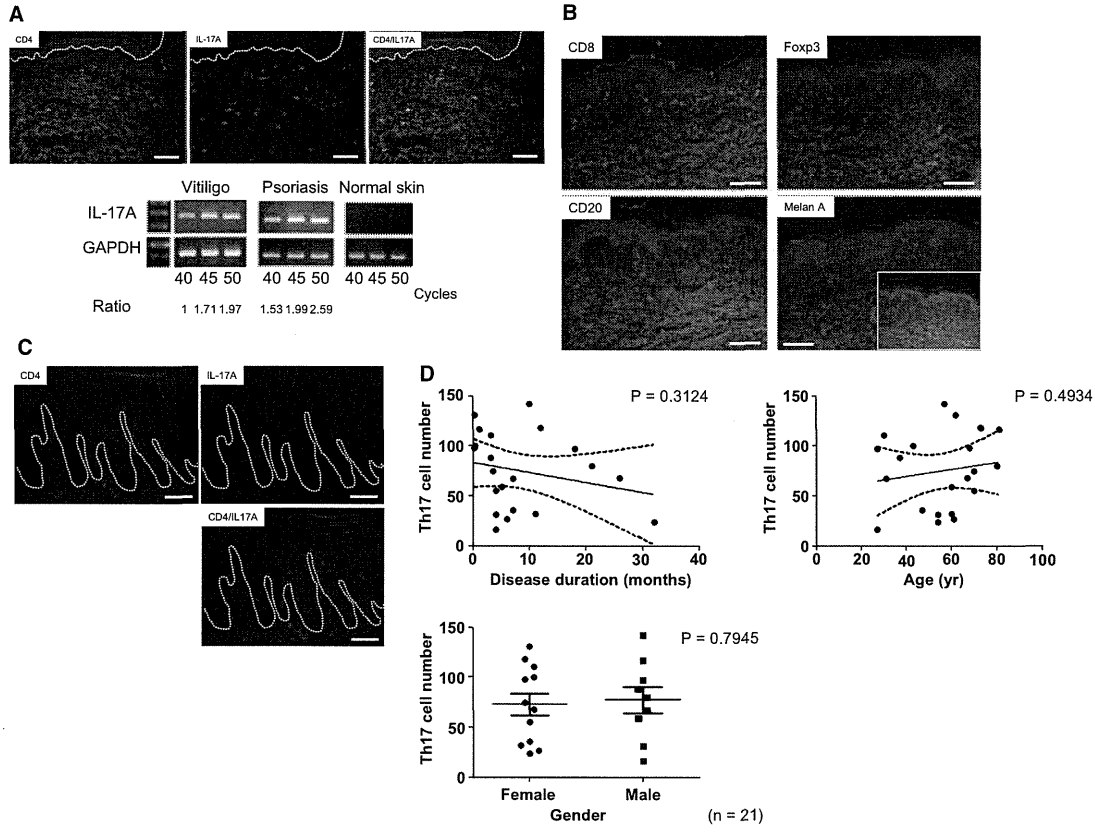

Figure 1. Photographic features of a representative generalized vitiligo patient and the immunohistochemical analysis for infiltrating cells in vitiligo skin. Multiple- and symmetrical-depigmented macules were present on the face and upper arm. A spindle-shaped skin specimen was obtained from the leading edge of an upper arm lesion. Immunostaining for CD4 and IL-17A in the vitiligo skin lesion indicated the significant infiltration of Th17 cells (yellow) positive for both CD4 (green) and IL-17A (red) mainly on reticular dermis and perivascular region. RT-PCR confirmed the same level of IL-17A expression in the vitiligo skin as in psoriasis skin (A). CD8-positive cytotoxic T lymphocytes (CTLs) (red, upper left) infiltrated the upper dermis and epidermis, whereas Foxp3 and CD20 positive cells (upper right and lower left) were only faintly detected. Melan-A-positive cells, highly differentiated melanocytes, were present in the normal region (lower right, small window), whereas they were absent in the vitiligo epidermis (lower right) (B). Psoriatic skin showed Th17 cell infiltration in the papillary dermis in addition to the epidermis (C). All images are original magnification ×40 for vitiligo and ×100 for psoriatic skin. The white bar indicates 100 μm. (D) The mean Th17 cell number present in vitiligo skin was counted on three independent fields, and the correlation with disease parameters such as disease duration, age, and gender was evaluated (n = 16).

nity to be infiltrated by Th17 cells, there was no significant correlation between the number of infiltrating Th17 cells and the clinical type, or with disease parameters such as disease duration, age, or gender in 21 patients with Th17 cell infiltration (Figure 1E).

Proinflammatory cytokines associated with Th17 cells influence in melanin activity

Because a significant number of Th17 cells were found in most of the vitiligo skin samples examined in this study, we hypothesized that there was a possible role for Th17 cell-related cytokines in melanocyte activity. Previous reports have shown that several cytokines downregulated tyrosinase activity through the activation of designated intracellular signaling pathways (Englaro et al., 1999; Kamaraju et al., 2002; Kholmanskikh et al., 2010). We therefore decided to examine the effects of IL-1β, IL-6, IL-17A, and IL-22, which are important cytokines induced by Th17 cell differentiation and maintenance, on melanocyte development and activity. MITF, a pivotal transcription factor related to melanocyte function and survival, expression and translocation was at first examined by immunocytochemistry (Figure 2A, C). Whereas there was apparent translocation of the MITF protein to the nucleus in untreated cultured melanocytes (Figure 2A), the MITF expression was decreased in the nucleus of the melanocytes treated with 10 ng/ml of IL-1β or IL-17A (Figure 2B, C), suggesting that there was a reduction in MITF-related signaling in melanocytes following cytokine treatment. In contrast, IL-22 treatment had no effect on melanocytes (data not shown), so we decided not to include IL-22 in the further experiments.

Next, we examined the expression of cytokine receptors by RT-PCR to confirm the ligand-to-receptor correspondence in melanocytes. Cultured human melanocytes were found to express IL-1R1, IL-6R, and IL-17RA without the addition of cytokines, whereas treatment with 10 ng/ml of their corresponding

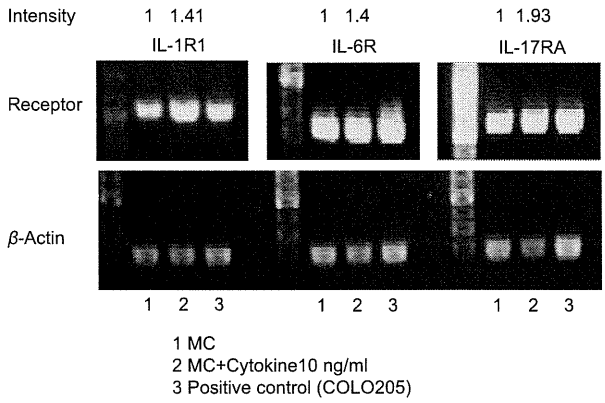

Figure 3. The expression of cytokine receptors in human melanocytes. IL-1R1, IL-6R, and IL-17RA mRNA were expressed in human melanocytes and were upregulated following treatment with their corresponding cytokines. COLO205 cells (colon cancer cell line) were used as a positive control. β-actin was used as a housekeeping gene.

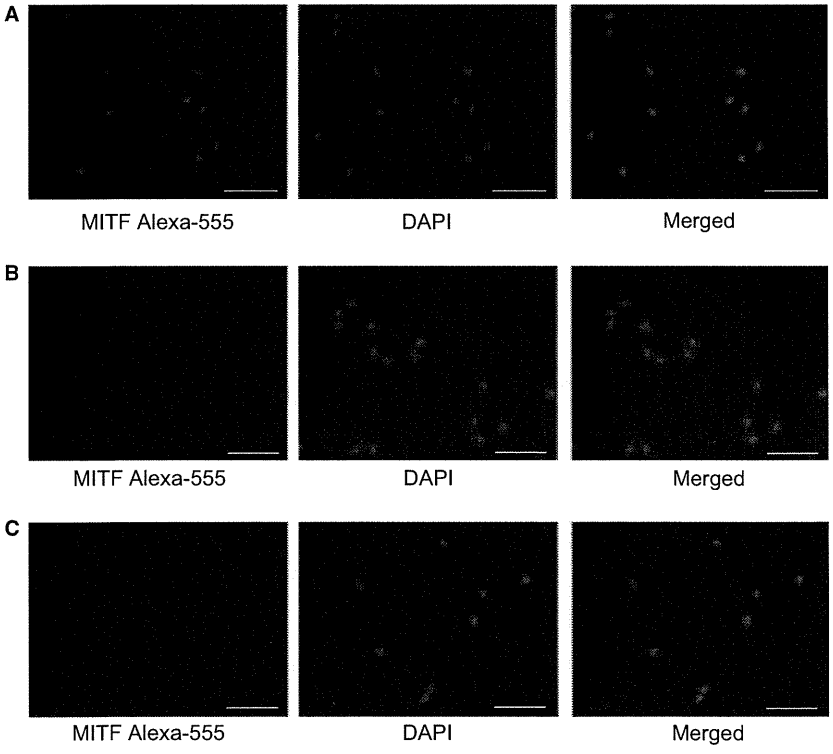

Figure 2. Immunocytochemical staining for MITF in human melanocytes. MITF was expressed mainly in the nuclei of untreated cells (A). In contrast, MITF expression was decreased after treatment with recombinant IL-1β (B) and IL-17A (C). The white bar indicates 50 μm.

cytokines increased receptor expression (Figure 3). COLO205 cells, the human colon cancer cell line expressing these receptors endogenously, were loaded in parallel with cultured melanocytes as a positive control.

To investigate the direct effects of Th17 cell-related cytokines on melanocytes in vitro, we examined the mRNA expression of melanogenic and melanocyte survival molecules after treatment of human melanocytes with recombinant human cytokines (Figure 4). The expression of *MITF*, which encodes a master transcription factor that regulates melanocyte function; of *TYR*, *TRP-1*, and *DCT*, which encode enzymes involved in melanin synthesis; and of *BCL2*, which encodes an anti-apoptotic protein, was measured by quantitative PCR. MITF expression was found to be significantly decreased in a dose-dependent manner after treatment with IL-1β, IL-6, and TNF-α (Figure 4A). The *MITF* transcription level decreased to <50% after treatment with 1 ng/ml of TNF-α. MITF was downregulated by 10 ng/ml IL-17A. In terms of the expression of its downstream enzymes, IL-1β significantly downregulated the genes, but only at a concentration of 10 ng/ml, whereas basic FGF upregulated their expression. IL-6 downregulated *TYRP1* and *DCT*, but there was no significant decrease in *TYR*. A 10 ng/ml concentration of IL-17A was needed to induce their significant downregulation. On the other hand, TNF-α significantly suppressed the expression of

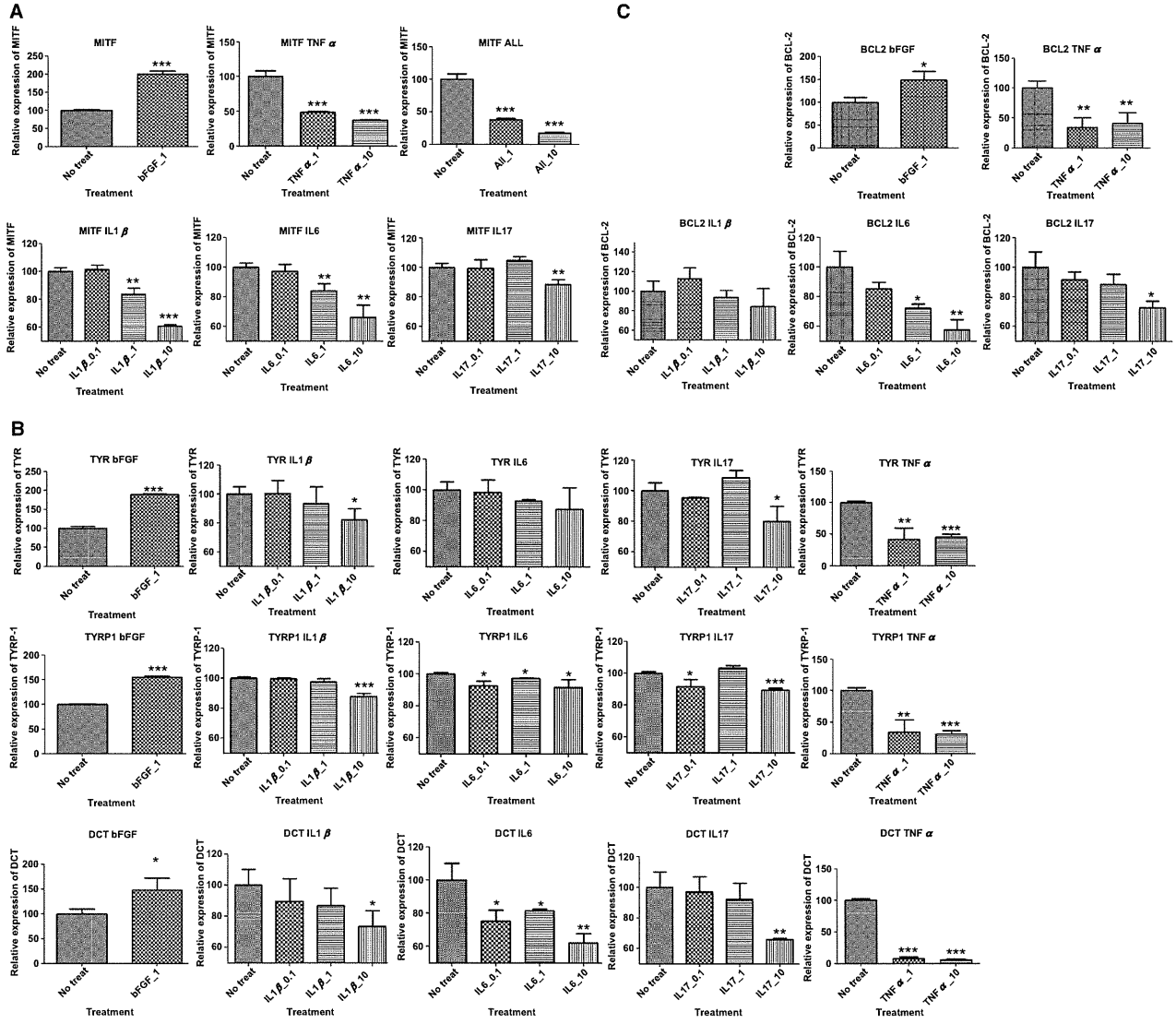

Figure 4. The quantitative analysis of the mRNA expression of MITF and genes encoding melanogenic enzymes. Human melanocytes were incubated with recombinant cytokines for 4 h at concentrations of 0.1, 1, or 10 ng/ml in the culture medium. The mRNA expression levels of MITF (A), genes encoding melanogenic enzymes (B), and B-cell lymphoma 2 (Bcl-2) (C) were measured by qRT-PCR. *P < 0.05; **P < 0.01; ***P < 0.001 compared with the expression level in untreated control cells.

these genes and *BCL2*, even at the concentration of 1 ng/ml, suggesting that TNF-α likely had the strongest suppressive effect on gene expression. BCL2 expression was decreased following treatment with IL-1β, IL-6, and IL-17A in a dose-dependent manner. Overall, there was a tendency for molecules related to melanocyte function to be downregulated following treatment with exogeneous cytokines (Figure 4B, C).

To determine the direct effects of Th17 cells on melanocytes, we performed coculture of the Th17 cells induced from peripheral blood mononuclear cells by an in vitro protocol with and without TGF-β treatment (Wilson et al., 2007) with melanocytes and real-time PCR. Th17-polarized cells without TGF-β decreased the expression of *MITF* and its downstream melanogenic molecules more than Th2-polarized cells did (Figure S1).

Furthermore, melanin production was measured after continuous treatment with exogenous cytokines including IL-1β, IL-6, IL-17A, and TNF-α. The percentage of melanin production was significantly lower in melanocytes treated with 1 and/or 10 ng/ml of exogenous cytokines than in untreated cells. In contrast, no reduction in total protein was observed after the addition of any of the cytokines (Figure 5). Because these cytokines are critical for the maintenance and development of Th17 cells from naïve $CD4^+$ T cells, we suggest that the presence of a specific local cytokine environment might be indispensable for Th17 cell recruitment and activation in vitiligo lesions, thereby indicating that they contribute significantly to depigmentation in addition to CTL (cytotoxic T cell) activation.

Production of cytokines by skin-resident cells

We have shown infiltration of Th17 cells in vitiligo skin and have demonstrated the inhibitory effects of Th17 cell-related cytokines on melanocyte function. As the cytokines examined in this study are produced not only by inflammatory cells but also by the surrounding cells, such as keratinocytes and fibroblasts, the source of the cytokine production was examined. We treated normal human epidermal keratinocyte (NHEK) and normal human dermal fibroblast (NHDF) cells with recombinant IL-17A and measured IL-1β, IL-6, and TNF-α production (Figure 6A, B). IL-17A exponentially increased the pro-

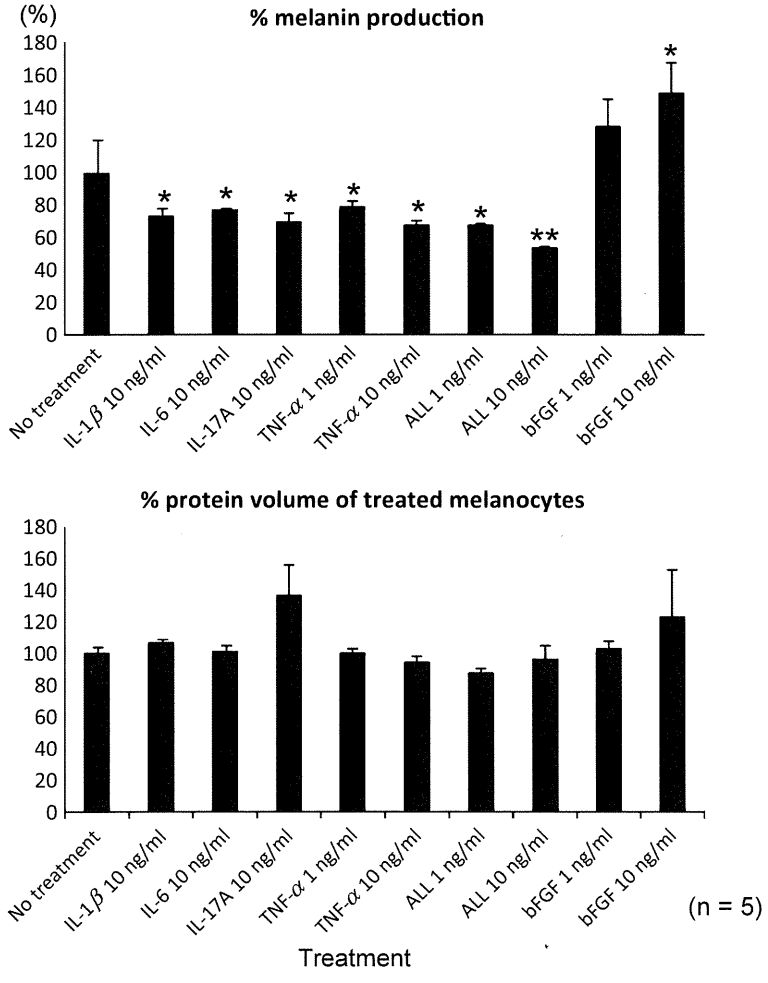

Figure 5. There is a decrease in melanin production after treatment with cytokines. Human melanocytes were incubated with 1 ng and/or 10 ng/ml of recombinant cytokines for 5 days in the culture medium (n = 5). Recombinant cytokines were added everyday. Cultured melanocytes were treated with 1 N NaOH and processed for absorbance at 450 nm to quantify the melanin volume. The protein volume of the cell extracts was measured to demonstrate whether the cytokines exerted the reduction of whole cell protein. *P < 0.05; **P < 0.01; ***P < 0.001 compared with the expression level of the untreated controls.